ARCHAEOMETRIC ANALYSES OF MURAL PAINTINGS FROM ANCIENT SIDE (ANTALYA) THEATRE GALLERY M

A THESIS SUBMITTED TO
THE GRADUATE SCHOOL OF NATURAL AND APPLIED SCIENCES
OF
MIDDLE EAST TECHNICAL UNIVERSITY

BY

SAADET KAYMAZ

IN PARTIAL FULFILLMENT OF THE REQUIREMENTS
FOR
THE DEGREE OF MASTER OF SCIENCE
IN
ARCHAEOMETRY

SEPTEMBER 2019

Approval of the thesis:

ARCAHEOMETRIC ANALYSES OF MURAL PAINTINGS FROM ANCIENT SIDE (ANTALYA) THEATRE GALLERY M

submitted by **SAADET KAYMAZ** in partial fulfillment of the requirements for the degree of **Master of Science in Archaeometry Department, Middle East Technical University** by,

Prof. Dr. Halil Kalıpçılar
Dean, Graduate School of **Natural and Applied Sciences** _____

Prof. Dr. Musa Doğan
Head of Department, **Archaeometry** _____

Prof. Dr. Mustafa Ümit Atalay
Supervisor, **Archaeometry, METU** _____

Assoc. Prof. Dr. Ali Akın Akyol
Co-Supervisor, **Conservation and Restoration of Cultural Properties, Ankara Hacı Bayram Veli University** _____

Examining Committee Members:

Prof. Dr. Musa Doğan
Biology, METU _____

Prof. Dr. Mustafa Ümit Atalay
Mine Engineering , METU _____

Assist. Prof. Dr. Alptekin Oransay
Archaeology, Anadolu University _____

Date: 09.09.2019

I hereby declare that all information in this document has been obtained and presented in accordance with academic rules and ethical conduct. I also declare that, as required by these rules and conduct, I have fully cited and referenced all material and results that are not original to this work.

Name, Surname: Saadet Kaymaz

Signature:

ABSTRACT

ARCHAEOMETRIC ANALYSES OF MURAL PAINTINGS FROM ANCIENT SIDE (ANTALYA) THEATRE GALLERY M

Kaymaz, Saadet
Master of Science, Archaeometry
Supervisor: Prof. Dr. Mustafa Ümit Atalay
Co-Supervisor: Assoc. Prof. Dr. Ali Akın Akyol

September 2019, 71 pages

In this study material of wall paintings were analyzed to determine the structure of plasters, mortars, and pigments of Side wall painting samples. Archaeometrical methods were used to investigate mineralogical and chemical compositions and raw material characterization. Binder-aggregate ratio and particle size distribution analysis, gravimetric analysis, petrographical thin section optical microscopy analysis, Raman Spectrometry, XRD, PED-XRF, SEM-EDX techniques and methods were used to examine the samples.

SEM-EDX analysis and Micro-XRF analysis indicate parallel results especially for iron (Fe) content of the samples. Iron (Fe) is the main element that plays a role in the formation of pink and red colors. As a result of thin section optical microscope analysis, wall painting samples could be divided into three different groups.

The main components in arriccio plaster layers are aggregates and binders. As a result of aggregate and binder analysis, arricio layer samples contain 63.32% percentage of aggregate regarding with average values. The aggregate structure of the samples is composed of very large, marine origin, rounded aggregates.

Keywords: Mural paintings, Archaeometry, Pigments, Raman Spectrometry, Side Excavations

ÖZ

ANTİK SİDE (ANTALYA) TİYATROSU M GALERİSİ DUVAR RESİMLERİNİN ARKEOMETRİK ANALİZLERİ

Kaymaz, Saadet
Yüksek Lisans, Arkeometri
Tez Danışmanı: Prof. Dr. Mustafa Ümit Atalay
Ortak Tez Danışmanı: Doç. Dr. Ali Akın Akyol

Eylül 2019, 71 sayfa

Bu çalışmada, Side duvar resmi örneklerinin sıva, harç ve pigment yapılarını belirlemek için içeriğindeki malzemeler incelenmiştir. Mineralojik ve kimyasal bileşimleri ve hammadde karakterizayonunu araştırmak için arkeometrik yöntemler kullanılmıştır. Bağlayıcı-agrega oranı ve partikül büyüklüğü dağılım analizi, gravimetric analiz, petrograik ince kesit optic mikroskopi analizi, Raman Spektrometresi, XRD, PED-XRF, SEM-EDX teknikleri kullanılarak örnekler tanımlanmıştır.

SEM-EDX analizi ve Micro-XRF analizi, özellikle numunelerin demir (Fe) içeriği için paralel sonuçları göstermektedir. Demir (Fe), pembe ve kırmızı renklerin oluşumunda rol oynayan ana unsurdur. İnce kesit optik mikroskop analizi sonucunda, duvar boyama örnekleri üç farklı gruba ayrılabilir.
Arriccio alçı katmanlarındaki ana bileşenler agrega ve bağlayıcıdır. Toplam ve bağlayıcı analizlerin bir sonucu olarak, arricio layer örnekleri ortalama değerlere göre% 63.32 toplam yüzde içermektedir. Numunelerin agrega yapısı çok büyük, deniz kökenli, yuvarlak agregalardan oluşmaktadır.

Anahtar Kelimeler: Duvar Resimleri, Arkeometri, Raman Specktrometresi, Side Kazıları, Pigmentler

To my family

ACKNOWLEDGEMENTS

I would like to thank my supervisor, Prof. Dr. M. Ümit Atalay and co-supervisior Assoc. Prof. Dr. Ali Akın Akyol, whose valuable support, advice, and especially encouragements caused to complete my thesis.

I am also grateful to Prof. Dr. Feriştah Alanyalı for her comments, providing materials and arcaheolocial context of my samples,and valuable suggestions during my studies. Also, I would like to send very special thanks to Prof. Dr. Sabri Alanyalı to permit for studying wall paintings from Side Excavations.

I am thankful to Prof. Dr. Yusuf Kağan Kadıoğlu, Emine Torgan and Kıymet Deniz for analyses.

My friends Gülşen Albuz Geren and Murat Eroğlu always helped to my studies and motivated me, their contribution to my study is a lot.

This study is supported by BAP, (Scientific Research Projects).

TABLE OF CONTENTS

LIST OF TABLES

TABLES

LIST OF FIGURES

FIGURES

CHAPTER 1

INTRODUCTION

1.1. Aim of the Study

The mural paintings have been studied abroad extensively regarding with its archaeological context or material composition. Some of those studies were summarized as follows:

The papers of Siddall offer detailed information on mural paintings' techniques, pigments and other materials. In her studies, mural paintings were analyzed with scientific techniques, mostly microscopic techniques. Siddall and others conducted a research on 57 fragments of wall painting excavated from the Temple of Venus (Pompeii). The team obtained some results using with analytical methods. As a results, pigments composed of natural earths, minerals and rare artificial pigments and both frescoe and lime painting techniques were adopted in paintings (Siddall 2006: 18-31; Piovesan et. al, 2011: 2633- 2634). Siddall also sork on mineral pigments in archaeology (Siddall 2018: 1-35).

There are many other publications on wall paintings in which archaeometrical methods were included. For example, Balandier and others applied some analysis on wall paintings found in Paphos (Cyprus). Consequently, frescoes have been identified and all the pigments were of mineral origin (Balandier et. al, 2017).

Raman analysis were preferred a lot for pigment studies of wall paintings. For instance, wall paintings from different sites of the Alcazar of Seville (Spain), (Perez-Rodriguez 2014: 602-609), Maya wall paintings in Ek'Balam (Mexico), (Vandenabeele 2005: 2349-2356), Romano-British wall paintings from Colchester and Lincoln (UK), (Edwards 2009: 553-560) were studied using with Raman spectroscopic analysis.

In Turkey several studies were carried out recently. A PHD thesis has been completed by Akyol in which material characterization of Zeugma mural paintings were determined. Several analytical techniques such as XRD, FTIR, SEM-EDX, Raman Spectroscopy, PED-XRF and physico-chemical techniques tests were applied the samples (Akyol et. al, 2005: 248-268; Akyol et. al, 2005: 91-100; Akyol et.al, 2004: 7-18; Akyol, 2009: 283 p).

A thesis study on wall paintings of Taxiarhis Church (Cunda Island, Ayvalık, Balıkesir) focused on conservational problems of historic wall paintings. Considering with this purpose, analytical techniques like XRF, SEM, and FTIR were used (Şerifaki, 2005: 77 p).

In another thesis study has been written by Demir, material characteristics of wall paintings from Anaia (Kadıkalesi) Church (Kuşadası, Aydın) were analyzed to reveal painting techniques and pigment characteristics (Demir, 2010: 84 p; Demir et. al, 2018: 39- 46).

Recently, another thesis study has been completed by Bilici provides an investigation to determine wall painting technique and material characterization of the pigments used in the samples from Saint Theodorus Trion church in the Cappadocia region (Bilici, 2018: 89).

In Cappadocia Region, there are some more archaeometrical studies on paintings like late Byzantine rock paintings research in Ürgüp (Santamaria et. al, 2009: 307-316) and late Ottoman mural paintings in Mustafapaşa- Ürgüp (Akyol and Kadıoğlu, 2008: 235-248).

Furthermore, a group of late Roman wall painting samples from Sinop Balatlar Church were analyzed to determine their material characteristics (Bakiler et. al, 2016: 263-273).

In Side, Eskici conducted a research on Side Harbour Baths wall paintings and plasters for the purpose of conservation (Eskici, 2004: 27-43).

This study was carried out to determine material characterization of plasters, mortars, and pigments of the mural painting samples. The samples were taken from Ancient Side Theatre's Gallery M foundations during sounding work in 2009 season.

In this study, several analytical techniques such as, XRD, SEM-EDX, PED-XRF, Raman Spectroscopy and physico-chemical tests had been used.

CHAPTER 2

GENERAL ASPECTS OF WALL PAINTINGS

2.1. Functions of Mural Paintings

Mural painting is the finishing layer or layers including plaster located on the wall (Akyol, 2009: 5). The surface for the wall paintings can be wall of a cave or wall of a building. There many early examples of rock paintings were found in Europe and Turkey like Cave Altamira paintings (Spain; ca 20000 BC), Cave Lascaux paintings (France; ca 18000 BC), Mounth Latmos paintings (Beşparmak Mountains, Aydın, Turkey; ca 6000 BC). On the other hand, as seen in Çatalhöyük (Çumra, Konya, Turkey; 7300-6000 BC) wall paintings, wall of the buildings was used for the paintings. Neolithic Çatalhöyük wall paintings were regarded as some of the first examples of prehistoric style painting associated with architecture (Figure 2.1a-d), (Çamurcuoğlu, 2015: 89).

Mural paintings accompanied with plaster serve significant functions in buildings and depending on those functions they store useful technological information. The main function of the plaster is to protect the masonry against weathering conditions, such as wetting and drying cycles, freezing and thawing cycles, salt crystallization cycles, due to the changes in ambient temperature, humidity conditions and wind flow. (Malinowski, 1981; Caneva et. al, 1991; Caner, 2003: 2; Akyol, 2009: 5).

Plaster keeps the masonry underneath healthy and durable against most weathering conditions. It may have several other functions such as the improvement of acoustical and thermal performance as well as the fire resistance of the wall (Callender, 1982; Caner, 2003: 2; Akyol, 2009: 7). The plasters in ancient masonry are known to affect the water vapor permeability of the walls through their "breathing property", letting the passage of water vapor through the wall. In

addition, plaster improves the appearance of the wall by hiding the imperfections of rough work and gives it an attractive texture compatible with the local environment (Houben and Guillaud, 1994). It can be said that survival of ancient buildings is because of choosing the building materials such as mortar and plasters are in the desired properties for their using purpose, their compatibility in properties with each other and with structural and architectural elements so they all form homogeneity in the building (Akyol, 2009: 7).

2.2. Historical Background of Mural Paintings

The history of the technique of mural painting is of interest to restorers, art historians, and also material scientist. Mural painting provides knowledge to identify the technique used to create the work that must be used to determine the essential technological and laboratorial examinations. Secondly, the history of mural painting technique qualifies the art historian with material data which is a useful contribution to the history of art itself. The determining of ancient techniques should be based on the combined data from literary sources, technological examination using archaeometrical methods (Mora et. al, 1984: 69, Akyol, 2009: 7).

The first known mural paintings appeared in Upper Paleolithic Period (about 30 000 BC). Those paintings are positive or negative imprints of hands applied to the walls of caves. Considering with cave paintings, the first method is evidently made by plunging the hand into a liquid coloring material (usually red earth or blood) in order to imprint its mark. The second method was still used recently by the Australian Aborigines. In this method, they coated the rocky surface with grease and then, by blowing through a tube, projected dry pigment powder around the hand. The pigment consists of red ochre in the earliest examples; later charcoal black was preferred (Mora et. al, 1984: 70-71).

It was the Magdalenian Period (20000-11000 BC in Europe) that Paleolithic rock painting reached its full development, as demonstrated by the masterpieces at Altamira and Lascaux Caves. Altamira cave paintings include 930 animal figures.

Besides drawings made with charcoal and scraping technique, most of them were made with paint. In Lascaux Cave around 2000 figures were discovered and most of them are animal figures (Windels, 1949: 69-99; Mora et. al, 1984: 71; Akyol, 2009: 8; Bingöl, 2015:17-18).

The principal pigments used in paleolithic period were natural oxides of iron and manganese, hematite and limonite, which provided a range of color from brown ochre to yellow, and to which were added black and sometimes white pigments. The pigments were finely ground and stored in shells, stones, or hollow bones and were applied to the wall with a binding medium consisting of grease, blood serum, urine, egg or milk (Obermayer, 1938: 111-119; Mora et. al, 1984: 71; Akyol, 2009: 8)

During the Neolithic period in Anatolia and Near East, people started to built structures either in the form of simple, domestic houses or special buildings with the aim of living in or for use as communal spaces. As a result, in the Neolithic Period (8000-5500 BC in Anatolia), paintings began to be associated with architecture (Figure 2. 2). The natural irregular surface of the rock was replaced by the flat surface of the wall with usually a clay rendering which served as a base for the painting (Akyol, 2009: 8; Çamurcuoğlu 2015: 64).

An important body of paintings from the beginning of the Neolithic Period (6000 BC according to C14 dating) has been discovered at Çatalhöyük in Çumra (Konya, Turkey), (Melaart, 1961; 41-65). A layer of mud or fine clay was applied to the walls of raw bricks held together by layers of mud and the paint was laid directly on this layer. The clay-based material which is rich in calcium carbonate content and it was analyzed to be “marl” in general, which is naturally available from the marl beds of the Konya Basin, extending underneath the site. Neolithic people of Çatalhöyük had sufficient skills and capability to use materials that can be obtained from around the settlement. Therefore, they created hard and white surfaces as supports for elaborate wall paintings (Akyol, 2009: 9; Çamurcuoğlu 2015: 80; Siddall and Çamurcuoğlu 2016: 482-488).

The analytical work showed that Çatalhöyük pigments mainly derived from common minerals and they were mainly inorganic based. The plasters (marl and soft lime) were most probably dry and already burnished when the paint was applied with water or organic binders the experimental work suggested that most possibly water and/or organic binders must have been used to fix pigments onto plasters. However, the poor durability of paint when used with water and plant-based oils was clearly evident during the experimental work. The evidence of surviving paintings after thousands of years may indicate that stronger organic binders might have been preferred for painting practices (Çamurcuoğlu 227-239).

The paintings of the beginning of the second millennium discovered in the Palace of Zimri-Lim at Mari (Figure 2.3) were executed directly on the mud rendering of the wall or on a surface rendering of mud and chopped straw covered with a thin whitewash of plaster, a technique which was used in the Neolithic paintings of Çatalhöyük (Figure 2.1f). The color was normally applied with a brush, but sometimes with a knife. In the second millennium, wall paintings of the Palace of Zimri-Lim at Mari were executed directly on the mud rendering of the wall or on a surface rendering of mud and chopped straw covered with a thin whitewash of plaster. The paint was usually applied with a brush, yet sometimes with a knife. The paintings of the palace of Yarim-Lim at Tell Atchana (Alalakh, Antakya, Turkey), which are roughly contemporary with the palace of Zimri-Lim at Mari, were executed on a lime rendering surface (Figure 2. 4). It consisted of a first layer or arriccio applied in one or two operations either directly onto the brick wall or onto a primary rendering of clay and pressed with the fingers to facilitate adherence. This was covered with a second thin layer of pure lime. Sometimes earth was added to the arriccio, which gave it grey in color; sometimes straw was added. The presence of fragments of calcite suggests that marble powder was also added as an inert charge. The colors were detected are black, red, yellow, blue, and grey-green. Remarkably, colors used here appear to be identical with those used for the Knossos frescoes (Figure 2. 5), (Wooley, 1955: 228-231, Akyol, 2009: 10).

The Knossos wall paintings composed of a layer of clay mixed with mud rubble, coated with a very dense surface rendering, was applied with impurities in two layers of calcium carbonate. Heaton stated that the painting was executed in fresco, having detected no traces of a medium. Thus, the major problem of the origins and early development of fresco painting is linked to the even more complex problem of ancient Greek mural painting, which has almost entirely disappeared (Heaton, 1910: 206-212; Mora et. al, 1984: 84; Akyol, 2009: 11).

In Anatolia, the evidence for mural painting during the Bronze Age (3000-2000 BC) is less abundant. Tiny fragments of painted plaster have been found in the Late Bronze Age levels of Troia (Çanakkale, Turkey), (Blegen, 1958: 76) and at the Hittite capital of Hattusa (Boğazköy, Turkey), (Bittel and Naumann, 1957: 17).

The Iron Age in Anatolia further contributes to wall paintings. The 8th-7th century BC fortified sites of the Urartian kingdom in eastern Anatolia have some paintings that combine stylistic aspects of Neo-Assyrian and Anatolian paintings. At Toprakkale (Van), traces of blue and red paint were discovered in a temple (Mellink, 1962: 80). Evidence for painting was also discovered at Altıntepe and Çavuştepe in Van region (Akyol, 2009: 10).

Archaic Period Lydian tumuli; Harta in Abidintepe/ Manisa (Mellink 1980: 91-98; Dededoğlu, 1996: 197-206) and Aktepe in Uşak (Yılmaz, 2008: 206) provide wall paintings in which human figures were depicted (Figure 2. 6). Exceptionally, Lydia presents a painted wooden tomb chamber from the Tatarlı Tumulus near Dinar in Afyon. In this case, no grounding layer was used, instead the painting was executed directly on the wood surface (Summerrer, 2005: 155-15; Emmerling et. al, 2010 :206). The paintings display a scene of battling soldiers that is reminiscent of Greek vase painting (Özgen, 1996: 73).

Polishing, first used to imitate marble, may have already been used for the plain backgrounds and the scenes with figures in the palaces of Pergamon, Antioch and Alexandria in the Hellenistic Period (4th-1st century BC). However, the general use

and systematic perfecting of the technique was applied specifically by Romans (from the 1st century BC). This contribution was closely related to the stylistic and ideological requirements of the interior decoration of Roman villas. The innovation of Romans was not the introduction of fresco painting but rather it was perfecting (Mora et. al, 1984: 89; Akyol, 2009: 12).

2.3. Principalities of Mural Paintings

The major components of mural paintings are the binder the aggregate and the pigments. The aggregate may also be called as filler. There is a direct relationship between the performance of mural paintings and properties of its components. Namely, components of mural paintings, clay, lime or gypsum as binder, different types of inorganic aggregates as filler, and organic and/or inorganic additives, directly impact on the performance of mural paintings (Torraca, 1969: 170-175; Wickens, 1984: 3-23; Martinez-Ramirez et. Al 1995: 39-50; Baronio et. al 1997: 41-46; Middendorf and Knöfel, 1998: 311-324; 1999; Casellato et. al, 2000: 217-232; Manzano et. al, 2000: 19-28; Siddall, 2000: 339-344; Young and Miller, 2000: 331-350; Tunçoku, 2001; Dheilly et. al, 2002: 155-161; Edwards et. al, 2002:277-281; Seabee et. al, 2003, Caner, 2003: 3; Siddall, 2006: 18-31; Akyol, 2009: 22).

Considering with materials and techniques in mural paintings, in most cases they are limited. For instance, because pigments must contain special properties there are only a small number of pigments can be used. There are some necessary conditions like being resistant to light and air and not being expensive. Besides, some stable pigments suffer extreme alterations in case of exposing to high humidity (Akyol, 2009: 22).

Mural paintings involve in a variety of techniques like fresco and secco. In fresco technique, which is the most important technique among others, the support involves in two layers. Fresco refers to any painting executed on a fresh lime intonaco layer whilst still moist, in such a way that the pigments are fixed by the carbonization of the lime included in the plaster ground (Mora et. al, 1984: 11). The first layer is a

rough initial layer which is called “arricio”. This initial layer applied on the wall as flat layer but not rendered meticulously. The arricio layer has two functions: to create a smooth layer and to provide a reservoir of humidity that is necessary for the “fresco reaction” (Akyol, 2009: 22).

On the other hand, the second layer is “intonaco” layer that is far finer and more flawlessly finished, typically even polished. It is wealthier in lime, mostly having a composition of two parts of fine-grained sand or marble dust to one part of slaked lime and is applied quite thinly (about 5-10 mm) (Akyol, 2009: 22).

The second significant mural painting technique is secco executed on a dry plaster using pigments mixed with a binder such as gum arabic or glue. Frequently, secco paintings are executed on a gypsum intonaco layer over a mud-based arriccio layer (Mora et. al, 1984: 12; Akyol, 2009: 26).

The earliest renderings that were destined to be painted were clay-base, sometimes simply smoothed down, and sometimes covered with white-wash to provide a uniform white ground. This white-wash might consist of fine clay such as kaolin, gypsum or lime, depending on the period in which it was executed (Mora et. al, 1984: 36).

2.3.1. Lime Renderings

The mortars and plasters as well as layers of mural paintings consist of binder and aggregate. Binder may be mud, gypsum or lime. Lime is obtained by roasting calcerous matter of any kind at high temperature (Akyol, 2009: 27).

Reaction is given below for CaCO3 (limestone);

$CaCO_3 (s) \rightarrow CaO (s) + CO_2 (g)$ $\Delta H = +176$ kJ (2.3)

Substances such as magnesium carbonate, clay, silica, oxides of iron etc. may be present and these affect the quality of the lime. The best lime for renderings and painting grounds is obtained from calcareous shingle or gravel from the bed of rivers (Mora et. al, 1984: 47-48; Akyol, 2009: 28).

Types of lime are fat lime or hydraulic lime depending on the amount of impurities in it. If the amount of impurities is less than 5%, the lime is named as fat lime, rich lime or high calcium lime. If the impurities exceed 5%, the lime is no more high calcium lime. Hydraulic limes can be further classified into several subgroups depending on the amount of impurities and its cementation index. Fat limes are obtained from the purer forms of limestone and they hydrate more easily than other grades (Boynton, 1980: 273-279; Holmes and Wingate, 1997; Akyol, 2009: 28).

Aggregates are those materials, natural or artificial in origin that is sufficiently fine to function as a rigid base for binder grounds. The common aggregates are sand, pozzolana, trass (volcanic minerals), powdered stone or marble and crushed brick. The size of the particles of the aggregates are very important, because it determines the number of vacuoles and consequently the quantity of binding material in the plaster (Figure 2. 7), (Mora et. al, 1984: 48-51, Akyol, 2009: 29).

The water used in preparing plaster (or mortar) must come from a clear fresh water source, free from organic impurities. The amount of water used in the rendering of binder and aggregate must not be excessive. A rendering prepared with too much water and applied to a slightly absorbent surface tends to become porous and has little resistance if it is not reworked. This is because the excess water upon evaporation creates spaces in the rendering while a compact crust forms on the surface (Mariani and Schippa, 1969: 231-236; Akyol, 2009: 29).

2.3.2. Pigments

If the visible portion of the solar spectrum is referred to as color, one understands by “pigment” a colored substance which, when ground and mixed with a suitable binding medium to a workable consistency, can be used in painting. The pigment, whether amorphous or crystalline, must be finely ground into uniform particles and it must remain insoluble in the medium (Mora et. al, 1984: 56-57, Akyol, 2009: 30).

The significance of a pigment can only be understood in relation to color absorption. What the eye sees as color is the remaining unabsorbed light. In addition, a

substance which absorbs all the rays of the sun is said to be black whereas one which reflects all of them is white; so, in a strictly physical sense, black and white cannot be described as colors. When sunlight is reflected almost but not completely, the effect

of grayness will occur. In this case, there has only been small absorption of light (Akyol, 2009: 30).

Pigments may be classified into three categories, such as mineral pigments; natural or artificial, organic pigments, natural (animal or vegetable) and synthetic, and mixed pigments. Natural pigments are found in the ground in the form of oxides, sulphides, carbonates, sulphates, etc. Their preparation is comparatively simple. After extraction, the mineral is dried in the sun, roughly ground, sieved to eliminate impurities and then ground to powder, cleaned and dried. Further grinding allows a finger granulation to be obtained if required. High quality pigments are obtained by further special sedimentation and drying processes in order to obtain still smaller particles (Mora et. al, 1984: 56-58; Akyol, 2009: 30).

Artificial mineral pigments are usually chemical products of well-defined composition which have been obtained by dry method, like cinnabar (produced by sublimation of Hg and S) or by wet method through precipitation of chemical solutions. The latter process is to be preferred because it produces pigments of excellent quality and very fine granulation. Natural organic pigments (animal and vegetable origin) are obtained from substances contained in some parts of animals from decoction or maceration of wood, fruits, leaves, bark or roots of plants. The coloring material is produced by evaporation and desiccation. Synthetic organic coloring substances may be dyestuffs, derivatives of aniline, phenols, quinines, etc. and although used in the production of colored fabrics, they are avoided in painting, even if of the best quality, because their resistance to light is definitely inferior to that of the mineral pigments. It should be noted that such synthetic coloring substances are sometimes used as cheap adulterants to enhance the appearance of

pigments which are otherwise perfectly reliable (Mora et. al, 1984: 57; Akyol, 2009: 31).

Mixed pigments may contain both mineral and organic material; examples are the so-called lake pigments made by precipitating an organic dyestuff on a colorless base, commonly an oxide or hydrate, so imparting its color to this base (Mora et. al, 1984: 57; Akyol, 2009: 32).

The most common red pigments in some Roman mural paintings was found to be hematite which is present in three forms; well crystallized, poorly crystallized and disordered hematite. Well crystallized hematite was most common described in ancient Roman text by Pliny used for the synopsis originated from Sinope. It was almost pure pigment but had different hues; blood red, ochre, deep brown and violet (Bearat and Pradell, 1997: 224;-225 Akyol 2009: 32):

The disordered hematite could be obtained by dehydration of goethite (yellow ochre) by heating it at temperatures lower than 850-900°C, above this temperature well crystallized hematite is produced. Its tint varies from orange and deep brown depending on the heating temperature (Akyol 2009: 32).

The predominant green pigments in Roman mural paintings are green earths and particularly celadonite. They were sometimes applying their green earth pigment over a yellow ochre undercoat to improve the adherence of the green paint to the lime plaster (Bearat and Pradell, 1997: 230-231).

Carbon is the most common coloring ingredient of black pigments, their consistency and minor constituents depending on the method of manufacture. Not only the scientific interest, but also the origins of the colors attracts the modern artists to use and manufacturers to produce them. Compositions of the pigments most of the time depends on necessity, raw material character or how it is produced related to its use in oil or water colour. For example, Indian yellow is prepared for the mainly magnesium euxanthate from cow's urine when animals fed on mango leaves, source India (Mora et. al, 1984: 56-68).

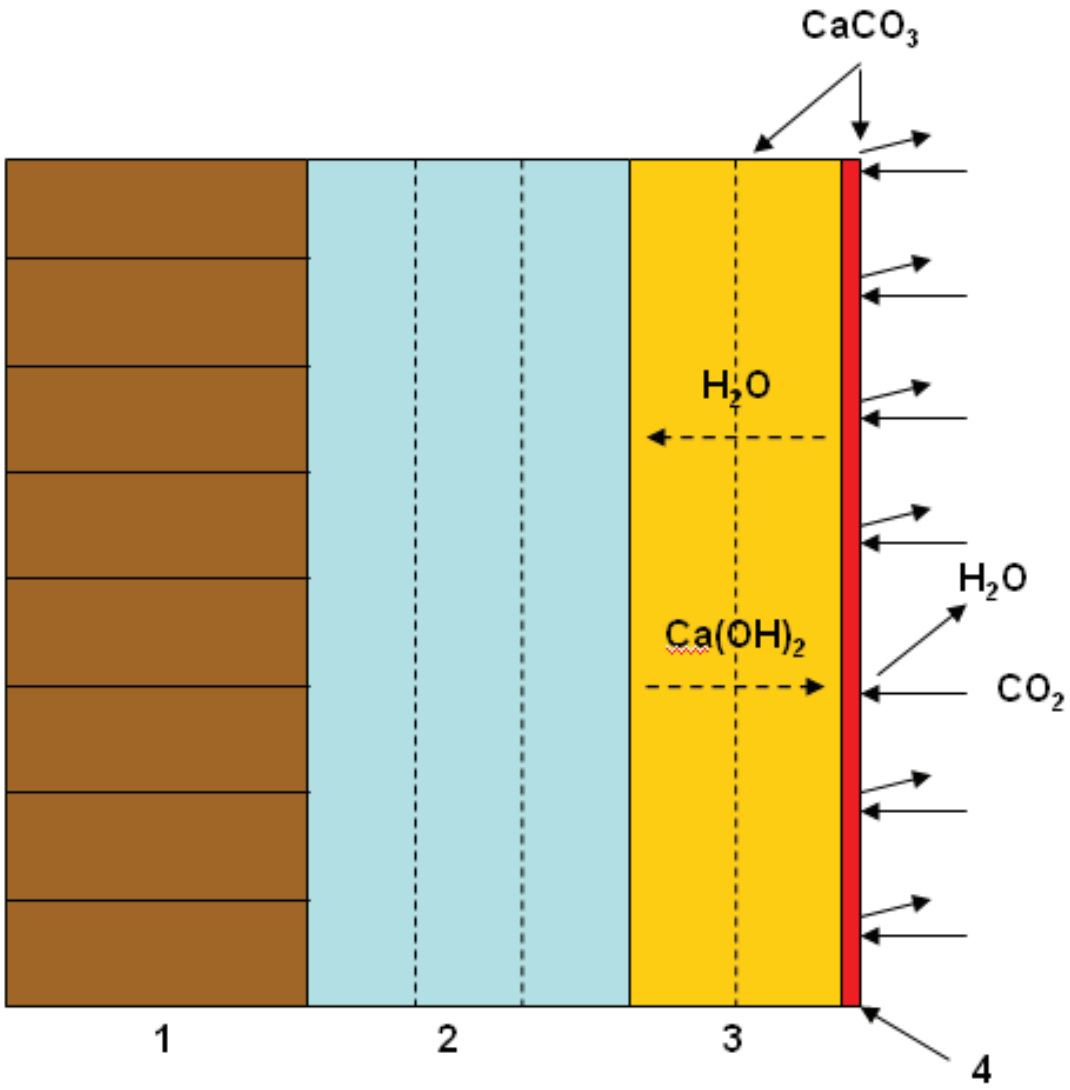

Figure 2.1. Frescoe Reaction (Akyol, 2009)

CHAPTER 3

ANCIENT SIDE

3.1. Location and Geography of Pamphylia and Side

The wide plain, which follows the seashore for more than 80 km from Manavgat to Antalya, was called Pamphylia in Antiquity (Figure 3.1), (Bean, 1997: 3). The region is bordered by the Taurus Mountains in the west and north, the Mediterranean Sea in the south and the Manavgat River in the east. The plain had been inhabited by humans since ancient times because of its fertile land irrigated by various rivers which are Katarraktes [Düdensu], Kestros [Aksu], Evrimedon [Köprüçay] and Melas [Manavgat River] (Figure 3.2), (Mansel, 1978: 1). Coastal areas of Pamphylia were invaded by the Aka's, which spread throughout the Eastern Mediterranean, in the 14th and 13th centuries BC. These various Greek tribes or clans called the region "the land of all tribes" (Mansel, 1978: 1-2). The name of Pamphylia emphasizes that the immigrants did not form themselves into local kingdoms, instead they prefer a clan organization (Grainger, 2009). On the western end of the Pamphylia, Lycia lies, to the north mountains appears and called Pisidia, to the east Rough Cilicia. (Figure 3.1), (Bean, 1997: 3). One of the important cities of Pamphylia is Side (Manavgat, Antalya) which is located on a peninsula 70 km east of Antalya (Figure 3.3 and 3.4). It was called as Selimiye District, in the last few years it was changed as Side. Moreover, in sources Side name can be seen as Satalia Vechia, Satalia Senex, Old Andaliya, Antaliya al-muhraqa (Burned Antalya), Old Antalya (Nolle, 1993: 38; Hellenkemper and Hild, 2004: 379; Soykal- Alanyalı, 2017: 187). The city was the most important port and coastal city of Pamphylia, especially before Atteleia was established. In ancient sources, it was written that Side was established by Kyme colonists coming from Aiollis Region (Mansel, 1978: 4). However, today there are several arguments about the establishment of the city.

Figure 3.1. Ancient Regions and Pamphylia

Figure 3.2. Ancient Pamphylia Region Borders (*Calder, W. M. ve G. Bean 1958)*

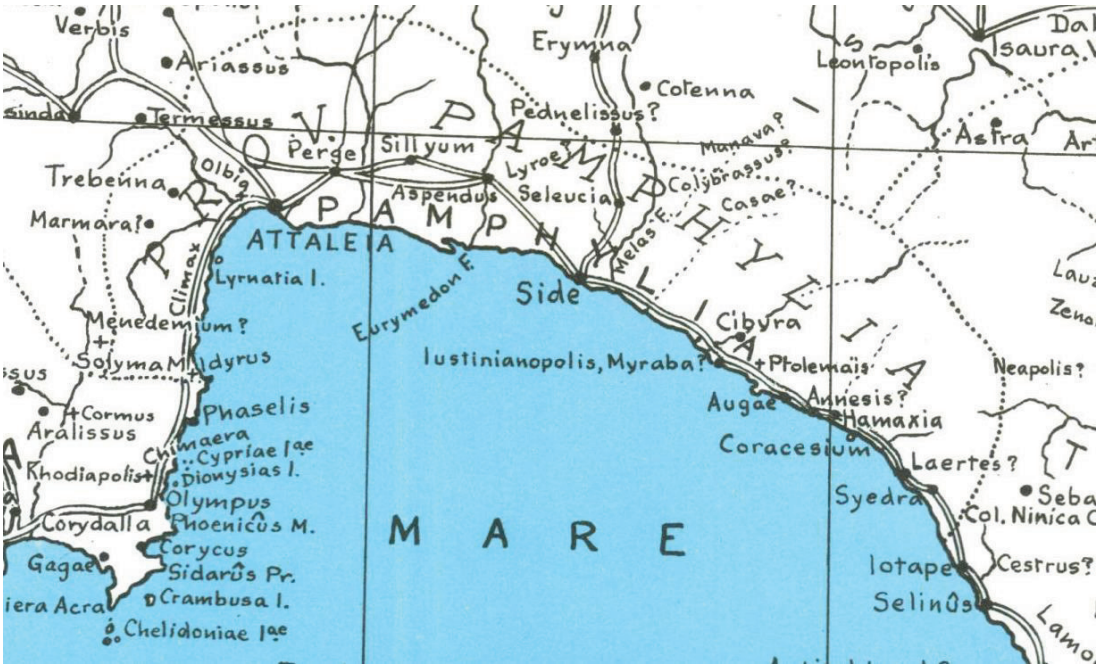

Mansel mentions that even if it is not certain Side was established 7. Century BC (1978: 4). The language of Side was different than Greek, Phonecian or any other. In the middle of 20. Century based on the documents it was determined that the language of Side belongs to Luvi language group. Considering with the documents including Side language it can be said that Side language was used until Hellenistic Period in Side (Soykal- Alanyalı, 2017: 188). The name of Side coming from Side language, it means pomegranate (Mansel, 1978: 9).

Figure 3.3. Antalya Gulf and Side Location

3.2. Research History of Ancient Side

Side attracted the attention of travelers and researchers arriving by sea, thanks to the theater and other magnificent monuments and it was marked on the sea maps (Mansel, 1978: 325). In Piri Reis's book Kitab-ı Bahriye, there is a map of Side and its surroundings (Mansel, 1978: 325). The first serious research was conducted by an

Figure 3.4. Side Peninsula Aerial Photo (Yıldırım, 2013)

English captain Fr. Beaufort in 1982. Beaufort prepared the plan of the city and defined some buildings and also with an inscription he found, he proved that the name of the city was Side (Figure 3.5), (Beaufort, 1818: 146-162; Mansel, 1978: 325). Shortly after Beaufort, Ch. R. Cockerell, M. Leake, and J.A. Cramer mentioned about Side in their publications (Mansel, 1978: 326). In 1842 yılında E.T. Daniel conducted some investigations in the city and results were published in the book of T.A.B. Spratt ve E.Forbes's who traveled to Side with him (Mansel, 1978: 327). Moreover, French researcher Ch. Texier made a summary of research history of Side in his book (Mansel, 1978: 327). In 1863 P. Tremaux visited the city and made plans and restitutions of the monuments of Side (Mansel, 1978: 327). In 1884 and 1885 K. Lanckoronski, archaeologist E.Petersen, and G.Niemann with a group of draftsmen and topographers conducted a detailed research in Pamphylia and Pisidia (Mansel, 1978: 327-328). Results of their study in Side with a city plan were place in the first volume of Lanckoronski's book (Figure 3.6), (Lanckoronski, 2005: 124-152). In 1900' H. Rott worked on Christian buildings of the city (Rott, 1908). In 1913, R. Paribeni and P. Romanelli visited the city and interested in inscriptions rather than monuments (Mansel, 1978: 328).

First scientific excavation work at Side was initiated by Arif Müfid Mansel in 1947 and continued without interruption until 1966 (Mansel, 1978: 328; İzmirligil, Atila, 2010: 63). Lots of monumental buildings were unearthed during the excavations and Mansel results were published as excavations reports, comprehensive articles, and books (Soykal- Alanyalı, 2016: 420). After Mansel, excavations continued by Jale İnan in 1966 until the unexpected death of Mansel in 1975. İnan's work was concentrated in the Great Bath (Soykal- Alanyalı, 2016: 420). After a break, excavations at Side were conducted by Ülkü İzmirligil from 1983 to 2008. The excavations under her direction were limited by only the theater and surroundings (Alanyalı, 2010: 94, Soykal-Alanyalı, 2016: 421). As of 2009, Side excavations has been taken over by Hüseyin Sabri Alanyalı on behalf of Anadolu University.

Figure 3.5. Captain Beaufort's Side City Plan (Beaufort, 2002

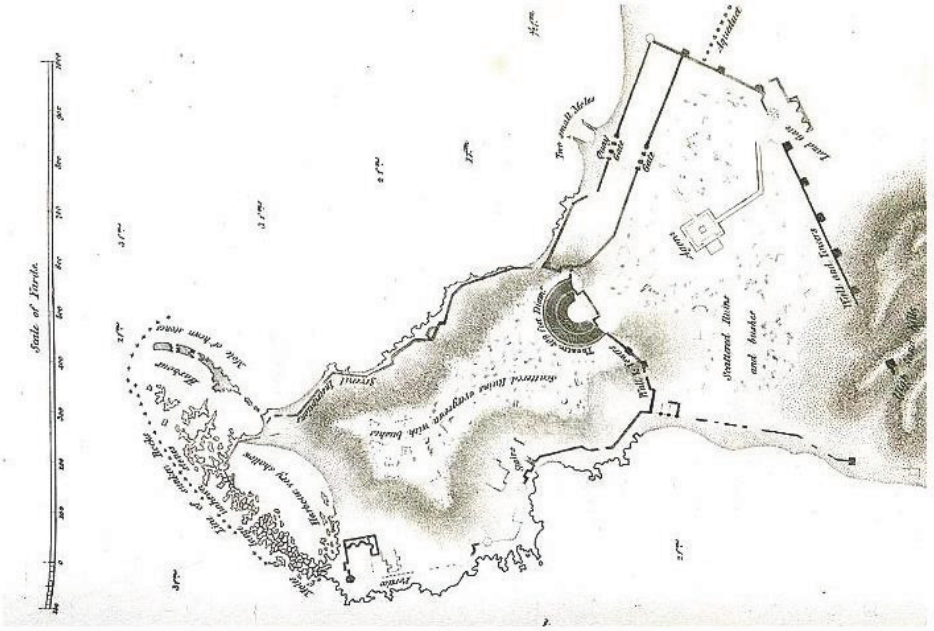

Figure 3.6. Lanckoronski's City Plan (Lanckoronski, 2005)

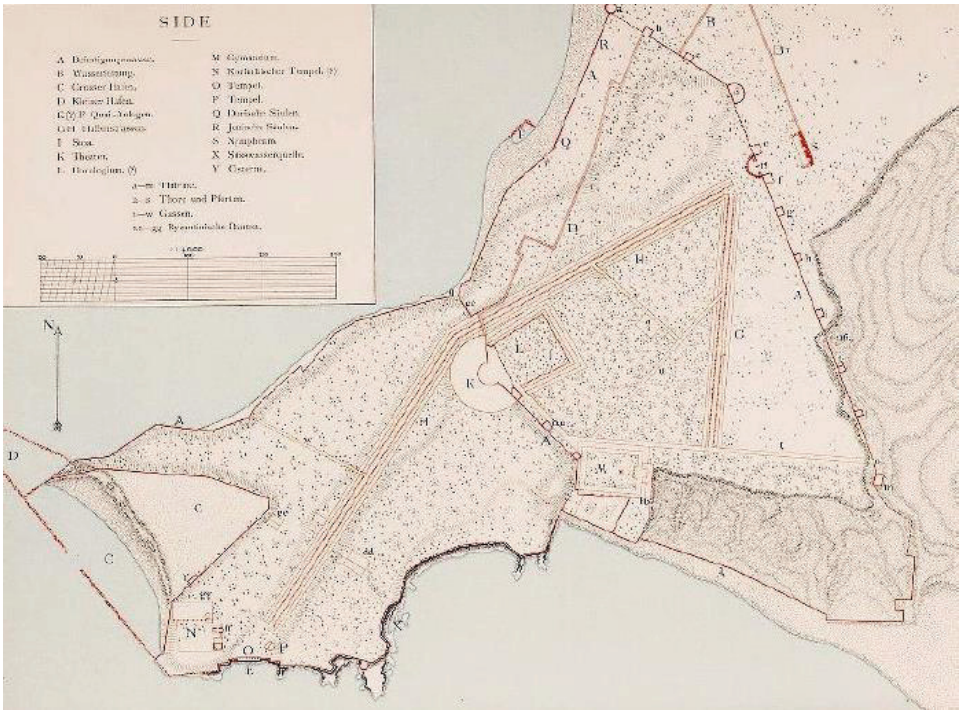

CHAPTER 4

MATERIALS AND METHODS

In this chapter, information about the samples studied and methodology for their investigation were given. Methods and tests used in this study were elucidated in detail separately.

4.1. Materials

Mural painting samples constitutes the sample group.

Before the analyses, sampling and documentation had been concluded that are explained given below.

4.1.1. Sampling

In this study, samples are the fragmented wall paintings which are taken from excavation house depot. In 2014, first group of samples were taken, and in 2015 examinations carried out in the excavation depot, the study material was re-handled, and another group of samples were selected.

Laboratory studies which include the basic compositional, mineralogical and chemical tests, and analyses were conducted in Historical Material Research and Conservation Laboratory (MAKLAB) at Hacı Bayram Veli University and Laboratory at Ankara University Earth Sciences Application and Research Center (YEBİM).

4.1.2. Nomenclature of the Samples

Nomenclature of the samples were carried out as follows; the first capital represents Side archaeological site (S). Second capital letter represents the abbreviation of the excavation in Turkish (Kazı). Third capital letter displays the abbreviation of thesis (T). Pigment samples were codded as SKT-P (Pigment) and plaster samples were codded as SKT-S (Sıva in Turkish), (Table 4.1).

Sample numbers are represented at the end of the code. For instance, SKT- P3 corresponds with the pigment sample belongs to Side Excavation Thesis samples.

Table 4.1. Codding

Sample Code	Material Descriptions
SKT-P	Pigment Samples
SKT-S	Plaster Layer (Sıva Katı) Samples

SKT (= **S**ide **K**azısı **T**ez çalışması)
Example : SKT-P1; First sample of the pigment layer
Example : SKT-S1ar; First sample of the arriccio layer of the plaster

4.1.3. Descriptions of Samples

Samples of the study include in wall painting fragments with pigments on the plaster. These samples were obtained from the foundations of Side Theatre's M Gallery during sounding work in 2009 (Figure 4.2).

Samples were taken from the boxes in which sounding material was kept based on sounding codes. 19 samples of the study come from Ancient Side Theatre Gallery M. Only one sample (SKT-18) comes from the Triumphal Arch and environs. This sample was kept for the study group as a representative sample. Most of the samples

belong to the boxes of K13-K16-K18. Considering with the ceramic findings that are found together with mural paintings point out to 3 th century AD. This group includes SKT-1, SKT-2, SKT-3, SKT-4, SKT-5, SKT-6, SKT-8, SKT-10, SKT-11 and SKT-14. There are two samples (SKT-9 and SKT-13) coming from K27 in which several mural paintings were found accompanying with animal bones and ceramic findings like pithos fragments. SKT-19 and SKT-20 samples belong to K24. Both K27 and K24 boxes indicate 4th century AD as terminus ante quem. SKT-12 sample belongs K78 and ceramic findings point out to 3 th century AD. SKT-15 sample comes from K30 in which in addition to mural paintings fragments several other materials like pieces of bricks, roof tile fragments, spindle whorls, metal slags and ceramic fragments were found. Ceramic findings indicate to in the middle of the 3 th century AD as the terminus ante quem. SKT-16 sample comes from K58 and SKT-17 comes from K59. Both boxes K58 and K59 includes ceramic findings dated to 3 th century AD. Lastly, SKT-18 comes from K90 in which a few ceramic findings were found including an LRD pottery body sherd (Alanyalı, 2009:7-25; Alanyalı, 2010: 95-96).

4.2. Methods

4.2.1. Documentation

The collected samples from Side were cataloged with details in the Table A.1 and Figures A.1 were registered. Moreover, detailed photographs of the samples were taken and given in Figures A2 in Appendix A.

The samples were codded so that analyses can be concluded safely. Thickness of arricio and intonaco layers were listed in the Table A.2 Besides, pigment layers of the samples were determined in the Table A.3.

4.2.2. Chromametric Analysis

Chromametric analysis is related with the identification of coloured samples. Colour identification was carried out by using a device (ColorQA PocketSPEC with Pro System III software) (Figure ..). The colors were identified by using CIELab color

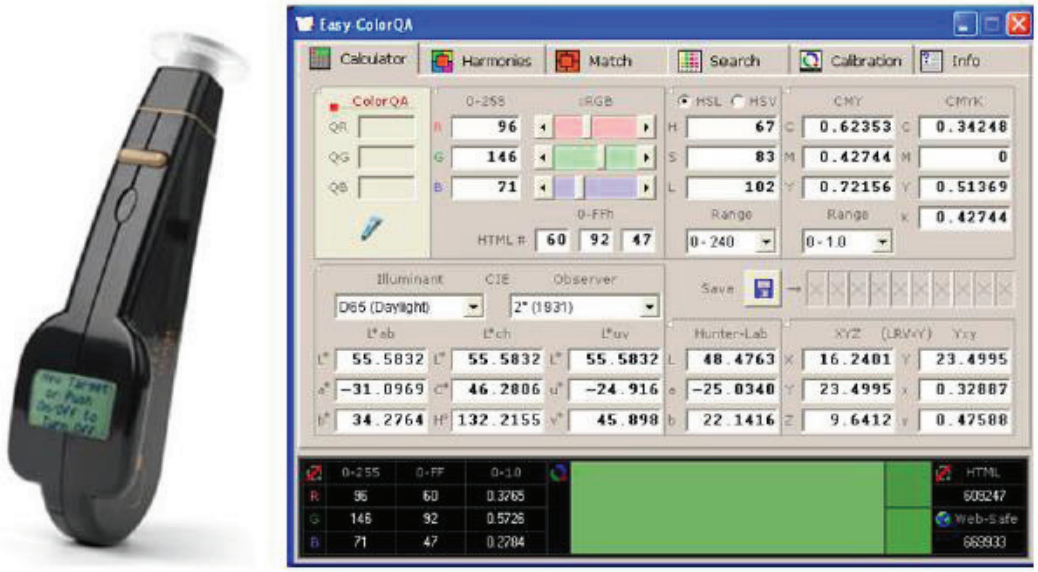

Figure 4.1. ColorQA Pro System III portable chromametry and its software

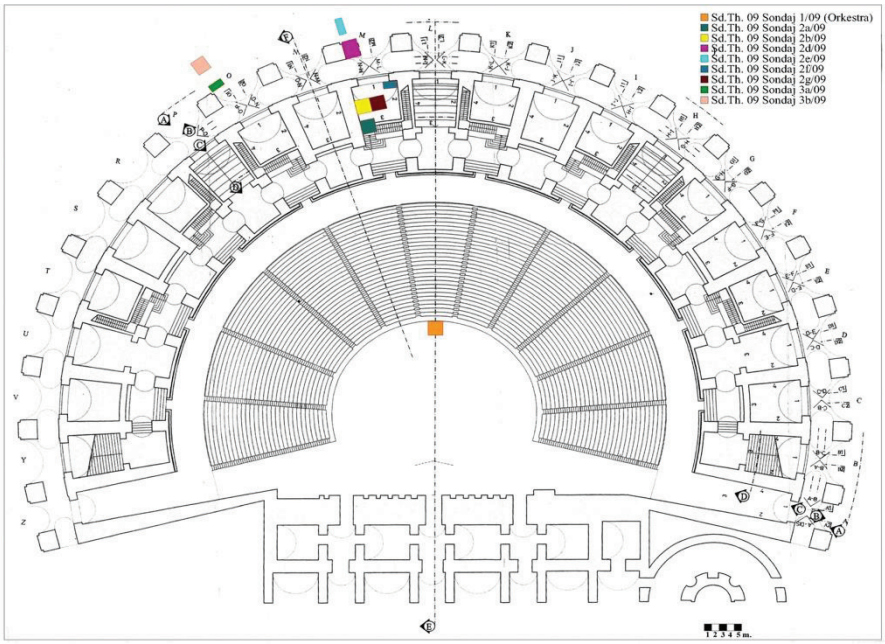

Figure 4.2. 2009 Theatre Soundings (Alanyalı, 2010)

systems. “L” is the lightness that measures the percentage of total solar spectral reflectance in relation to a pure white surface; “a” and “b” are measures of the degree red/green and yellow/blue in quantity. In the measurement, whiteness test for calibration was first carried out. Then, the measuring was carried directly on the surface of the samples. Chromametric analysis was applied to the pigment layers of the mural painting samples (Akyol, 2009: 53; Kaymaz et. al, 2017: 446). The chromametric measurement results were given in Table 4.1.

Figure 4.3. Soundings of 2009 (Side Excavation Archieve).

Table 4.2. *Enter the Table Caption here*

Örnekler	L	a	b	Görünen Renk
SKT-P1	7,24	27,02	8,17	Kırmızı
SKT-P2	48,65	8,39	35,86	Pembe
SKT-P3a	4,55	-0,71	0,86	Siyah
SKT-P3b	36,89	43,61	24,46	Kırmızı
SKT-P3c	47,99	-1,55	36,71	Sarı
SKT-P3d	76,93	-6,38	25,27	Beyaz
SKT-P4	42,10	15,96	40,47	Pembe
SKT-P5a	37,91	-28,66	29,77	Yeşil
SKT-P5b	7,87	24,31	12,34	Kırmızı
SKT-P5c	5,06	0,001	-0,001	Siyah
SKT-P5d	57,56	-10,82	39,45	Sarı
SKT-P6	9,63	15,37	14,77	Kırmızı
SKT-P7a	6,77	0,001	-0,002	Siyah
SKT-P7b	89,88	0,005	-0,010	Beyaz
SKT-P8	13,57	27,24	15,50	Kırmızı
SKT-P9a	81,72	-4,93	14,46	Beyaz
SKT-P9b	23,38	33,03	28,84	Kırmızı
SKT-P10	49,34	-30,85	21,78	Yeşil
SKT-P11a	57,81	10,66	57,05	Sarı
SKT-P11b	19,30	25,05	18,56	Kırmızı

4.2.3. Determination of Raw Material Composition

The binder and aggregate ratio and particle size distribution of aggregates were determined with respect to the structure of the raw material.

4.2.3.1. Determination of Binder/ Aggregate Ratio

Plasters and mortars are usually formed of two components, one is “aggregate” that is mainly silicates and silicon dioxide and it is acid insoluble. The other is “binder” that is mainly calcium carbonate and it is acid soluble. In order to find out the percentages of aggregate and binder parts, the weighed dry samples (Msamp) were treated with 5% HCl solution to decompose all carbonates present (Jedrzejevska, 1981: 311-329; Middendorf and Knöfel, 1990: 75-92). Insoluble parts were filtered, and residue was washed with distilled water until all chloride ions are removed. It was checked by treating a drop of filtrate with dilute and acidic AgNO3 solution. If chloride was removed, no white turbidity was observed (Akyol, 2009: 57).

Samples were dried in an oven and weighed. Percent of acid soluble and insoluble parts were calculated using following formula:

Insoluble % = [(Weight of the sample – Weight of the aggregates) / Weight of the sample] x 100

Acid Soluble % = 100 – Insoluble %

4.2.3.2. Determination of Particle Size Distribution of Aggregates

The distribution of the particle size of a sample indicates to the proportions of different particle sizes it includes. The proportions are generally depicted by the relative numbers of within specified size classes or by relative weights of such classes. The term fractionation in soil or soil related materials such as plasters and mortars refer to any process used to sort the material particles into distinct classes according to size. Sieving and sedimentation are the most common methods. In this study, the sieving method was used (Black et. al, 1965: 1584; Akyol 2009: 58).

Sieving is a convenient procedure for segregated particles coarser than 0.05 mm. The probability of a particle passing a given sieve at a given time of shaking depends upon the nature of the particle and the properties of sieve (Akyol 2009: 58).

There are two types of sieving that are wet and dry. In this study, dry sieving was preferred to apply. First of all, sieves were arranged in the sequence 1000, 500, 250, 125 and 63 μm from top to bottom (Means and Parcher, 1963). The weighed sample put the shaker and separates were transferred. The accumulated weighth was compared to total weight of the coarse fractions previously determined.

In this study, Udden-Wentwort grain size classification (Wenworth, 1922: 377-392) was preferred (Table 4.2).

Table 4.2. *Udden / Wentworth grain size classification scheme*

Size (µm)	Wentworth Size Class		Rock Type
(256 - 4096) x 10^3	Boulder	Gravel	Conglomerate / Breccia
(64 - 256) x 10^3	Cobble		
(4 - 64) x 10^3	Pebble		
2000 - 4000	Granulate		
1000 - 2000	Very coarse sand	Sand	Sandstone
500 - 1000	Coarse sand		
250 - 500	Medium sand		
125 - 250	Fine sand		
62.5 - 125	Very fine sand		
31 - 62.5	Coarse silt	Silt	Siltstone
15.6 - 31	Medium silt		
7.8 - 15.6	Fine silt		
3.9 - 7.8	Very fine silt		
0.06 - 3.9	Clay	Mud	Claystone

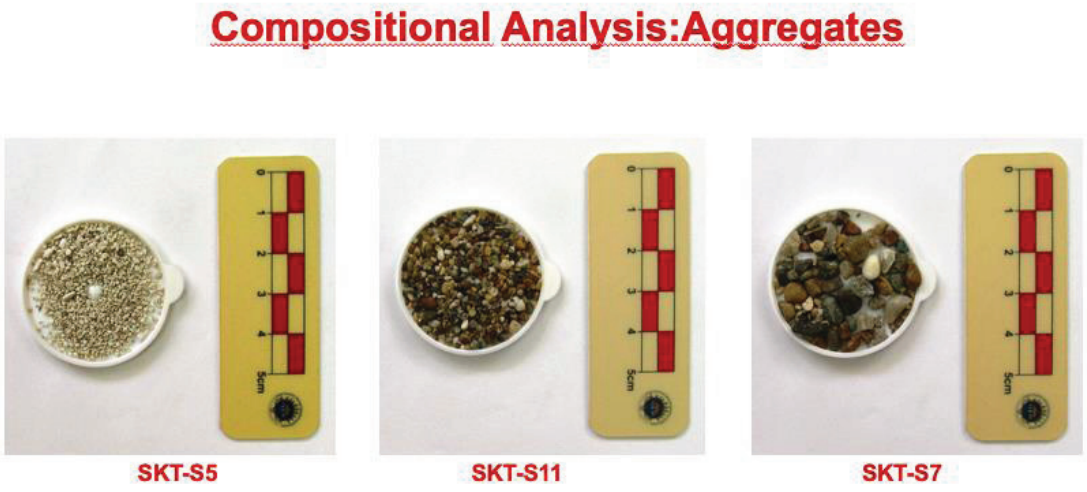

Figure 4.4. Aggregates after asidic treatment

4.2.4. Gravimetric Analysis (Loss on Ignition- LOI)

The method preferred in this study is similar to the method by Dean (1974: 242-248) that is the modification process described by Galle and Runnels (1960: 603-618). In this study process followed was given below:

From a powdered sample (grain size <63 μm) about 1 gram was weighed accurately (up to 0.1 mg precision) and dried in an oven at 100-110°C in a pre-weighed porcelain crucible to get constant weight (which is generally obtained by keeping the crucible in the oven at 100-110°C overnight). After cooling in a desiccator to room temperature, the sample and crucible were weighed. The weight difference gave the dry weight of the sample. The difference between original and dried sample gave water content of the sample. Dry weight of the sample was the basis for all weight loss calculations. The sample and crucible were then placed in a muffle furnace and heated to 500°C for one hour. After cooling to room temperature, the sample was weighed again. The difference between this weight and the dry weight is the amount of organic carbon ignited. Heating was repeated at least twice. The sample was returned to the muffle furnace and heated to 950°C for one hour. The weight loss between 500-950 °C is the amount of CO2 evolved from carbonate minerals. Again heating was repeated at least twice.

In this analysis, mural paintings' layers were processed individually.

4.2.5. Thin Sections and Polarized Optical Microscopy

Considering with mineral phases and textural structure of samples, thin section is a very crucial for the study. Comparing with other analyses makes it results most meaningful. Support from XRD, differential thermal analysis, chemical analysis should be obtained (Black et. al, 1965: 1584; Kerr, 1977: 442; Rapp, 2002: 326).

Observation of the thin sections was carried out by using reflected and transmitted light. Examinations of thin sections should proceed from lower to higher power in both plain and cross polarized light (Black et. al, 1965: 1584; Akyol, 2009: 64).

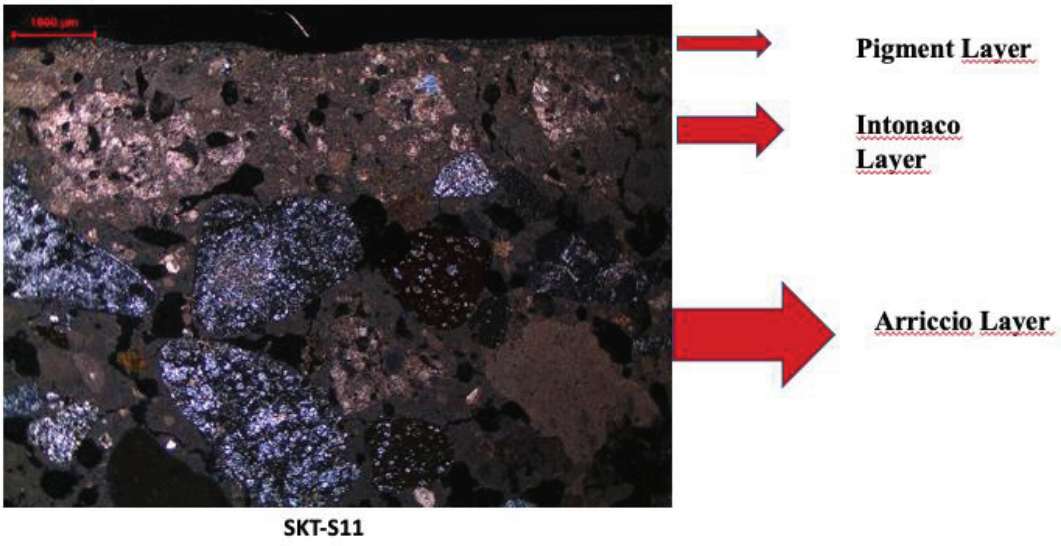

Figure 4.4. Thin Section Optical Microscopy exhibits three layers of the mural paintings

In the preparation of thin sections, usually a thin sections slice is cut from the material, sufficiently large to be a representative sample. One of this slice is polished with progressively finer grades of abrasive until perfectly flat and smooth. The polished face sticked to a glass slide with a proper adhesive (Hodges, 1964; Akyol, 2009: 64).

In this study, thin sections of wall painting samples (including arricio and intonaco plaster layers) were prepared and examined under optical microscope. LEICA Research Poliarizan DMLP Model optical microscope was used in the investigations. Photographs were taken with LEİCA DFC280 digital camera connected to the microscope and evaluations were made using Leica Qwin Digital Imaging Program (Kerr, 1977: 442; Rapp, 2002: 326; Kaymaz et. al, 2016: 105).

Table 4.3. Petrographical thin section optical microscope (aggregate/binder) analysis

Sample Groups	Total Aggregate/ Binder Ratio		Matrix Binder Composition (100%)				Matrix Aggregate Composition (100%)		
	Agg (%)	B (%)	Lime	M/Ls	Clay	Gp	M & R Fragments*	BP	Org.
Group 1 / Intonaco	35	65	100	-	-	-	100 (Q,Ls,C,Ch)	-	-
Arricio Layer	65	35	90	-	10	-	98 (Q,Ls,Op,Qs, Pl,Sr,R,Ch,F)	2	-
Group 2 / Intonaco	5	95	100	-	-	-	100 (Q,Ls,By)	-	-
Arricio Layer	12	88	55	-	10	35	100 (Q,Ls,Op,Pl,Py,Ch)	-	-
Group 3 / Intonaco	45	55	100	-	-	-	100 (Q,Ls,C,Ar,F,Op,Ch)	-	-
Arricio Layer	18	82	90	-	10	-	95 (Q,Ls,St,Qs,Op,Ch)	-	5
Group 4 / Intonaco	35	65	100	-	-	-	100 (Q,Ls,By,Op)	-	-
Arricio Layer	40	60	55	-	15	30	98 (Q,Ch,By,A,Pl,Op)	-	2
Group 5 / Intonaco	40	60	55	-	15	30	98 (Q,Ch,By,A,Pl,Op)	-	2
Arricio Layer	22	78	85	-	15	-	99 (Q,C,By,St,Cs,Op)	1	-

(*) Notations: A: Andesite, Ar: Aragonite, B: Basalt, BP: Brick Particles, By: Biotite, C: Calcite, Ch: Chert, Cs: Claystone, F: Fossil, Gp: Gypsum, Ls: Limestone, Op: Opaque Minerals, Org: Organics, Pl: Plagioclase, Py: Pyroxine, R: Radiolarite, Q: Quartz, Qs: Quartzite, St: Sandstone, Sr: Sericite

Group 1: SKT-S1, SKT-S2, SKT-S3, SKT-S4, SKT-S6, SKT-S7, SKT-S8, SKT-S9, SKT-S10, SKT-S11,

SKT-S13, SKT-S14, SKT-S15, SKT-S16, SKT-S17, SKT-S20

Group 2: SKT-S5

Group 3: SKT-S12

Group 4: SKT-S18

Group 5: SKT-S19

4.2.6. Micro X-Ray Fluorescence Analysis (Micro-XRF)

The chemical composition of the pigment layers of the wall painting samples was determined and documented by means of Micro-XRF analysis. SPECTRO brand MIDEX-M model micro-XRF device was used in the analysis. The device is used for chemical analysis in mineral, rock or any solid, liquid, powder, film samples.

4.2.7. X-Ray Fluorescence Analysis (PED-XRF)

In X-ray fluorescence (XRF) spectrometry the material being examined is irradiated with X-rays, and as a result the atoms of each element emit a characteristic radiation of a particular wavelength. The emitted radiations are then separated by a diffraction crystal and can be detected and measured either by a photographic plate or by a geiger counter (Akyol, 2009: 66)

X-ray fluorescence spectroscopy is a nondestructive technique used in the study of works of art. It is a relatively widely used technique for the analysis of artifacts, since it is relatively rapid, cheap, sensitive, and specific (Salmon, 1970: 31-46; Felici et. al, 2004: 17-25; Ferretti, 2000: 285- 286; Akyol, 2009: 66)

Considering with mural paintings, the XRF measurements are one of the main techniques to find out the use of pigment due to the presence of the caharactersitic elements (Aloupi et. al, 2000: 18-24; Felici et. al, 2004: 17-25; Akyol, 2009: 66).

The chemical contents pf the arricio layer of the mural painting samples were determined by PED-XRF analysis (Shackley, 2011). In this study, SPECTRO X-lab 2000 model PED-XRF spectrometer was used. USGS (United States Geological Survey) standards and GEOL, GBW-7109 and GBW-7309 were used as a reference. The chemical content of the samples obtained by PED-XRF analysis was evaluated also with Cementation Index (Boynton, 1980) data on Lime types and strength properties. (Kaymaz et. al, 2016: 105).

4.2.8. Scanning Electron Microscopy (SEM-EDX)

In this study, elemental composition of four different regions selected from mural paintings sample layers were analyzed by scanning electron microscope (SEM) and connected XRD analyzer (SEM-EDX) ZEISS brand EVO 40 model SEM-EDX device was used. Using with this device, solid or powder samples with diameters between 9-15 mm and thickness between 0.1-30 mm can be examined. In the scanning electron microscope technique, the surface is scanned with an electron beam and the interactions with the surface produce a high-resolution image. As a result of the electron beam, various signals are formed on the surface; these are back-scattered, secondary and Auger electrons and X-ray fluorescence photons and other photons of various energies. By detecting these species released from the surface by suitable detectors, element composition as well as surface morphology can be determined (Akyol, 2009: 69; Ataman, 2012: 87-96; Kaymaz et. al, 2017: 447-448).

4.2.9. Raman Spectroscopy

This analysis was named after the Indian physicist who first observed it in 1928, Sir Chandrasekhara Venkata Raman. As a non-destructive method. Raman spectroscopy can reveal the chemical composition and structure of objects of archaeological and historical importance in order to determine their authenticity, provenance, and technology. The technique brings together studies from different areas and so the importance of the technique can be increased day by day (Edwards and Chalmers, 2005).

Raman technique is suitable for many organic and inorganic archaeological materials in the form of solids, liquids, polymers or vapors. One of the main areas of Raman Spectroscopy is identification of pigments. Several Raman spectroscopy studies on pigments from paintings have been performed especially in order to support other techniques. Micro Raman spectroscopy not only an excellent technique to identify inorganic pigments but also allows the characterizations of organic media

(Brysbaert and Vandenabeele, 2004: 689-692; Edwards and Chalmers, 2005; Akyol, 2009: 71; Vandenabeele, 2013).

In the analysis, Horiba Jobin Yvon LabRam Confocal Raman Spectrograph with an Olympus BX41 microscope and Peltier cooling CCD (1024 X 256 pixels) dedector was used to acquire Raman spectra. The samples were analyzed without any previous mechanical or chemical treatment being undertaken. Microscopic images of the sample area observed prior to the spectral collection with the position of focal point for each spectrum were taken by a Raman PCI model video camera (Akyol, 2009: 72).

In the study, different colored pigments (red, pink, green, yellow and black) were examined under Raman confocal microscope.

CHAPTER 5

RESULTS AND DISCUSSION

The wall painting samples obtained from the soundings carried out in 2009 from the galleries of the Side Theater (Gallery M); after being documented with different layers (arricio, intonaco, and pigment layers) it was started to be examined with different analyzes on plaster and pigment layers.

Examinations on Side wall paintings began with giving codes for nomenclature and catalogued (Table 5.1). Afterwards, for documentation samples were photographed individually accompanied by a scale (Figure 5.1). Furthermore, wall painting fragments' layers, arricio (lower plaster layer) and intonaco (finish coat of plaster) were determined and measured separately (Table 5.2 and Figure 5.1).

The pigment layer of the mural samples is mostly red, then pink, black and white, and green and yellow. Afterwards, chromametric analysis was applied to see the precise color differences and the tone differences were shown in numerical values (Figure 5.2).

The main components in arriccio plaster layers are aggregates and binders. Wall painting arricio plaster layers were acidic treated, aggregates obtained (carbonate-free) were weighed and total aggregate / binder ratios of the samples were ascertained. With the application of aggregate and binder analysis, the entire structure with carbonate content, which is purified by acid in the plaster, is expressed as "binder". As a result of aggregate and binder analysis, arricio layer samples contain 63.32% percentage of aggregate regarding with average values (Tablo 5.4). The aggregate structure of the samples is composed of very large, marine origin, rounded aggregates.

The size distribution of aggregates of arricio layers of the samples was determined using with six different sizes of sieve. Wall painting arricio plaster samples (except for SKT-S5ar) indicate similarities in terms of aggregate particle size distributions.

SKT-S3-P3 Pigment Layer **SKT-S3 Arricio Layer** **SKT-S3 Section: All layers: Arricio, Intonaco and Pigment**

Figure 5.1. Description of the Samples

Small stone fragments and very coarse sand size (> 1000) aggregates in the plasters are 75,03%, fine / average / coarse sand size aggregates (63-1000) are 24,01% and silt /clay aggregates are 0,96%. The coarse sand constitutes the main structure of aggregate content of the samples (Tablo 5.5). Regarding with SKT-S5ar, its aggregate distribution is composed of small/ medium/ coarse and very coarse sand (Wentforth, 1922).

Petrographic optical microscope analysis of thin sections of wall paintings' arricio and intonaco layers were obtained. Considering with arricio and intonaco layers' binder and aggregate content, distribution of particles and types samples could be divided into three different groups (Tablo 5. 6). The total matrix aggregate (TMA)

content of plaster layers are range between %12-55 for arricio layers while range between %5-45 for intonaco layers. The binder structure of arricio layers included mixed of lime and lime/ clay and lime/ clay/ gypsum, the binder structure of intonaco layers consist of lime in all the samples. Among the three thin section sample groups, Gr3's aggregate content includes %5 percentage of organic materials (straw, plant fibers), (Tablo 5.6).

The chemical composition of arricio layers of the samples was determined by SEM-EDX analysis (Tablo 5.7). Chemical composition of the samples consists of CaO (avr. %42,68), LOI (total carbonate; avr. %40, 40) and SiO_2 (avr. %10,09). As expected, it was revealed that plaster layers' content of lime and carbonate (LOI) ratio is very high. Regarding with chemical compositions samples demonstrate a homogenic structure yet, SKT-S5ar differentiates strikingly with its main/ trace element (especially very high SO_3). Similarly, when arricio layers of the samples classified into groups (Triangle Plotting); SKT-S5ar acquires a different character with its content, other samples constitute a closely related heap (Figure 5.3).

Arricio layers of the samples were evaluated with Cementation Index (CI) value (Boynton, 1980), (Table 5.7). CI can be expressed as the ratio of the acid-soluble portion of the samples to the portion alkaline-soluble.

Two different analyzes showed parallel results especially for iron (Fe) content of the samples. Iron (Fe) is the main element that plays a role in the formation of pink and red colors. Samples which show a generally homogeneous structure differ with the existence of some elements. For example, the Ti and V content in the SKT-P1 sample distinguishes this sample from the others.

Table 5.1. *Cataloging*

Samples	Location	Material	Sounding	Box No.	Color
SKT-1	Side Theatre M Gallery	Fresco	2b/09	K13- K16- K18	Red
SKT-2	Side Theatre M Gallery	Fresco	2b/09	K13- K16- K18	Pink
SKT-3	Side Theatre M Gallery	Fresco	2b/09	K13- K16- K18	Red, yellow, white, black
SKT-4	Side Theatre M Gallery	Fresco	2b/09	K13- K16- K18	Pink
SKT-5	Side Theatre M Gallery	Fresco	2b/09	K13- K16- K18	Without pigment layer
SKT-6	Side Theatre M Gallery	Fresco	2b/09	K13- K16- K18	Green, red, cream
SKT-7	Side Theatre M Gallery	Fresco	2b/09	K35	Red
SKT-8	Side Theatre M Gallery	Fresco	2b/09	K13- K16- K18	Black dots on white
SKT-9	Side Theatre M Gallery	Fresco	2b/09	K27	Red
SKT-10	Side Theatre M Gallery	Fresco	2b/09	K13- K16- K18	Red, cream
SKT-11	Side Theatre M Gallery	Fresco	2b/09	K13- K16- K18	Green
SKT-12	Side Theatre M Gallery	Fresco	2f/09	K78	Yellow, red
SKT-13	Side Theatre M Gallery	Fresco	2b/09	K27	Red
SKT-14	Side Theatre M Gallery	Fresco	2b/09	K16	White
SKT-15	Side Theatre M Gallery	Fresco	2b/09	K30	Yellow?
SKT-16	Side Theatre M Gallery	Fresco	2a/09	K58	Yellow, black, white, red, green
SKT-17	Side Theatre M Gallery	Fresco	2a/09	K59	White, pink?
SKT-18	South of the Theatre	Fresco	3a/09	K90	Red, black
SKT-19	Side Theatre M Gallery	Fresco	2b/09	K24	White
SKT-20	Side Theatre M Gallery	Fresco	2b/09	K24	White

REFERENCES

Akyol, A.A**.,** Demirci, Ş., Kadıoğlu, Y.K. ve Türkmenoğlu, A.G., (2005). Zeugma Arkeolojik Alanı A Bölgesi Duvar Resimleri Analizleri: Birinci Aşama, T.C. Kültür ve Turizm Bakanlığı Kültür Varlıkları ve Müzeler Genel Müdürlüğü 26. Uluslararası Kazı, Araştırma ve Arkeometri Sempozyumu, 24-28 Mayıs 2004, Konya, Türkiye, 20. Arkeometri Sonuçları Toplantısı, T.C. Kültür ve Turizm Bakanlığı Yayın No: 3032 / Kültür Varlıkları ve Müzeler Genel Müdürlüğü Yayın No: 105, s. 91-100.

Akyol, A.A., Demirci, Ş., Kadıoğlu, Y.K. and Türkmenoğlu, A.G. (2005). Zeugma Arkeolojik Alanı A Bölgesi Duvar Resimleri Analizleri: Birinci Aşama, 20. Arkeometri Sonuçları Toplantısı, T.C. Kültür ve Turizm Bakanlığı Yayın No: 3032 (105), 91-100.

Akyol, A.A., Demirci, Ş., Kadıoğlu, Y.K. and Türkmenoğlu, A.G. (2006). Zeugma Arkeolojik Alanı A Bölgesi Duvar Resimleri Önincelemeleri -Oda C13 – Preliminary Examinations of Wall Paintings of Zeugma Archaeological Area Sector A Room C13, International Symposium on Zeugma: From Past to Future (20-22 May, 2004, Gaziantep), 7-18.

Akyol, A.A. (2009). Material Characterization of Ancient Mural Paintings and Related Base Materials: A case Study of Zeugma Archaeological Area, Archaeometry Department of METU, Unpublished PHD. Thesis in METU.

Akyol, A.A. and Kadıoğlu, Y. K. (2008). Ürgüp Mustafapaşa Aziz Georgios Kilisesi Arkeometrik Çalışmaları. 23. Arkeometri Sonuçları Toplantısı. Dösim Basımevi. Ankara.

Alanyalı, H.S. Side Kazısı 2009 Yılı Sezonu Yayımlanmış Kazı Raporu.

Alanyalı, H.S. (2010). Side Tiyatrosu ve Çevresi 2009 Yılı Çalışmaları, ANMED, 94-103.

Alanyalı, H. S. (2010). Side Tiyatrosu ve Çevresi 2009 Yılı Çalışmaları. *ANMED*, (8), s.94- 103, 2010.

Aloupi, E., Katydas, A.G., and Paradellis, T. (2000). Pigment Analysis of Wall Paintings and Ceramics from Greece and Cyprus: The optimum Use of X-Ray Spectrometry on Specific Archaeological Issues. X-Ray Spectrometry (29), 18-24.

Baker, M.T., von Endt, D., Hopwood, W., and Erhardt, D. (1998). FTIR microspectrometry: A Powerful Conservation Analysis Tool, The American Institute for Conservation of Historic and Artistic Works, Preprints of Papers Presented at the 16th Annual Meeting, New Orleans, Louisiana, June 1–5, American Institute for Conservation of Historic and Artistic Works: Washington, D.C., Rosenberg, S.Z. (Eds.), 1-13.

Bakiler, M., Kırmızı, B., Ormancı Öztürk, Ö., Boso Hanyalı, Ö., Dağ, E., Çağlar, E., Köroğlu, G. (2016). Material Characterization of the Late Roman wall painting samples from Sinop Balatlar Church Complex in the black sea region of Turkey. Microchemical Journal 126. 263-273.

Balandier, C., Joliot, C., Menager, M., Vouve F., Vieillescazes, C. (2017). Chemical Analyses of Roman Wall Paintings Recently Found in Paphos (Cyprus). *Journal of Archaeological Sciences.* Vol. 17. 332-339.

Bean E. G. (1999). *Eskiçağda Güney Kıyılar*, çev. İ. Delemen, S. Çokay, Arion, İstanbul.

Beaufort, F. (1817). Karamania: or, A brief description of the south coast of Asia-Minor and of the remains of antiquity. With plans, views, &c. collected during a survey of that coast, under the orders of the Lords commissioners of the Admiralty, in the years 1811-1812. London.

Beaufort, F. (2002). Karamanya, çev. A. Neyzi, D. Türker, Suna- İnan Kıraç Akdeniz Medeniyetleri Araştırma Enstitüsü, Antalya.

Béarat, H., Fuchs, M., Maggetti, M. and Paunier, D. (1997). Roman Wall Painting: Materials, Techniques, Analyses and Conservation, Proceedings of the International Workshop, Fribourg 7-9 March, 1996, Institute of Mineralogy and Petrology, Fribourg University

Bilici, B. (2018). Kapadokya Aziz Theodoros Trion Kilisesinin Duvar Resimlerindeki Pigmentlerin Arkeometrik Yöntemlerle İncelenmesi. Pamukkale University. Unpublished Master Thesis.

Bingöl, O. (2015). *Arkeolojik Mimaride Resim*. Bilgin Kültür Sanat Yayınları. İstanbul.

Bittel, K. and Naumann, R. (1957). Boğazköy. 3, Funde aus den Grabungen 1952 – 1955, Berlin: Mann, 17.

Black, C.A., Evans, D.D., Ensminger, L.E., White, J.L., Clark, F.E. (1965). Methods of Soil Analysis, No. 9 in the Series Agronomy, American Society of Agronomy:Crop Science Society of America : Soil Science Society of America, Wisconsin.

Blegen, C. (1958). *Troy 4: Settlements VIIa, VIIb and VIII*, Princeton University Press.

Boynton, R.S. (1980). *Chemistry and Technology of Lime and Limestone*, 2nd Edition, John Wiley & Sons, New York.

Bosch, E. C. (1957). *Pamphylia Tarihine Dair Tetkikler* (Antalya Bölgesinde Araştırmalar No. 1), Türk Tarih Kurumu Yayınlarından, V. Seri, No.17, Ankara.

Callender, J.H. (1982). *Time Saver Standards for Architectural Design Data*, McGraw-Hill Book Company.

Caner, E. (2003). Archaeometrical Investigations of Some Seljuks Plasters, Unpublished M.S. Thesis in METU.

Caneva, G., Nugari, M.P. and Salvadori, O., (1991). Biology in the Conservation of

Works of Art, ICCROM, 182 p.

Casellato, U., Vigato, P.A., Russo, U. and Matteini, M., A (2000). Mössbauer Approach to the Physico-Chemical Characterization of Iron-Containing Pigments for Historical Wall Paintings, Journal of Cultural Heritage 1, 217- 232.

Cennini, C.A. (1960). The Craftsman's Handbook: The Italian "Il Libro Dell arte", Translated by D.V.Thomson Jr., Dover Publication Inc., New York.

Çamurcuoğlu, D, (2015). The Wall Paintings of Çatalhöyük (Turkey): Materials, Technologies, Artists, Institue of Archaeology, UCL, Unpublished PHD. Thesis.

Davey, N. (1961). *A History of Building Materials*, Camelot Press, London.

Dedeoglu, H. (1996). Harta Abidintepe Tümülüsü Kazı Çalısmaları, ArkDer IV, 197-206.

Demir, S., Şerifaki, K., Böke, H. (2010). Geç Dönem Bizans Kilise Yapısında Bulunan Duvar Resimlerinin Özellikleri Kuşadası Kadıkalesi Anaia. 5. Ulusal Yapı Malzemesi Kongresi ve Sergisi. İstanbul.

Demir, S., Şerifaki, K., Böke, H. (2018). Execution technique and pigment charactersitics of Byzantine wall paintings of Anaia Church in Western Anatolia. Journal of Archaeological Science: Reports 17. 39-46.

Dheilly, R.M., Tudo, J., Sebaibi, Y. and Queneudec, M. (2002). Influence of Storage Condition on the Carbonation of Powdered Ca(OH)2, Construction and Building Materials 16, 155-161.

Edwards, H.G.M, Chalmers, J.M. (2005). Raman Spectroscopy in Archaeology and Art History, RSC Chemistry Spectroscopy Monographs Series, Royal Society of Chemistry, Publishing, Cambridge, UK.

Edwards, H.G.M., Middleton P.S., Hargrevas, M.D. (2009). Romano-British Wall Paintings. Spectromichia Acta. Volume 73.Issue 3. 553-560.

Eskici, B. (2004). Wall Paintings and Plasters of Side Harbour Baths: Techniques, Problems, and Conservation Methodology. Anadolu/ Anatolia 27. 27-43.

Felici, A.C., Fronterotta, G., Piacentini, M., Nicolais, C., Sciuti, S., Vendittelli, M., and Vazio, C. (2004). The Wall Paintings in the Former Refectory of the Trinita` dei Monti Convent in Rome: Relating Observations from Restoration and Archaeometric Analyses to Andrea Pozzo's own Treatise on the Art of Mural Painting, Journal of Cultural Heritage 5, 17-25.

Jedrzejevska, H. (1981). Ancient Mortar as Criterion an Analysis of Old Architecture, Proceedings of Symposium on Mortars, Cements and Grouts Used in the Conservation of Historic Buildings, ICCROM, Rome, Italy, pp. 311-329.

Hild, F. and Hellenkemper, H. (2004). Tabula Imperii Byzantini 8: Lykien und Pamphylien. Verlag der Österreichischen Akademie der Wissenschaften.

Holmes, S. and Wingate, M. (1997). *Building with Lime, A Practical Introduction*, Intermediate Technology Publications, London.

Houben, H. and Guillaud, H. (1994). *Earth Construction*, Intermediate Technology Publications, London.

Kaymaz, S, Ü. Atalay, and Akyol, A.A. (2016). Side Tiyatrosu Duvar Resimlerinde Arkeometrik Ön Çalışmalar, KST 31, Erzurum, 103-118.

Kaymaz, S, Ü. Atalay, and Akyol, A.A. (2017). Side Tiyatrosu Duvar Resimlerinde Arkeometrik Çalışmalar, Uluslararası Genç Bilimciler Buluşması II: Anadolu Akdenizi Sempozyumu (2015), 445-449.

Kerr, P.F. (1997). Optical Mineralogy, Mc Graw-Hill Book Company, New York.

Lanckoronski, K.G. (2005). *Pamyhlia ve Pisidia Kentleri*. 1848-1933. Suna & İnan Kıraç Akdeniz Medeniyetleri Araştırma Enstitüsü. İstanbul.

Malinowski, R. (1981). Ancient Mortars and Concretes; Durability Aspects, Mortars, Cements and Grouts Used in the Conservation of Historic Buildings, Proceedings of Symposium in Rome, 341-350.

Mansel, A. M. (1978). *Side, 1947-1966 Yılları Kazıları ve Araştırmalarının Sonuçları*. Ankara: Türk Tarih Kurumu.

Manzano, E., Bueno, A.G., Gonzales-Casado, A. and del Olmo, M. (2000). Mortars, Pigments and Binding Media of Wall Paintings in the 'Carera del Darro' in Granada, Spain, Journal of Cultural Heritage 1, 19-28.

Mariani, E. and Schippa, G. (1969). Technologia dei Materiali, in: Mora, P., Mora, L. and Philippot, P., Conservation of Wall Paintings, Chimica Applicata, Edn. Siderae, Rome, 231-236.

Martinez-Ramirez, S., Puertas, F., Blanco Varela, M.T. (1995). Carbonation Process and Properties of New Lime Mortar with Added Sepiolite, Cement and Concrete Research 25 (1), 39-50.

Mellaart, J., (1962). Excavation in Catal Huyuk, First Preliminary Report 1961,

Anatolian Studies 12, 41-65.

Mellink, M. (1962). Archaeology in Asia Minor, American Journal of Archaeology

66 (1), 80.

Middendorf, B., Knöfel, D. (1990). Use of Old and Modern Analytical Methods for the Determination of Ancient Mortars in Northern Germany, Proceedings of the 3rd Expert Meeting, Hamburg, NATA-CCMS Pilot Study on Conservation of Historic Brick Structures, Berlin, 75-92.

Mora, P., Mora, L. and Philippot, P. (1984). *Conservation of Wall Paintings,* Butterworths, ICCROM, Glasgow, England.

Nolle, J. (1993). Side im Altertums. Inschriften griechischer Stadte aus Kleinasien 43, Bonn.

Obermayer, H. (1938). Probleme der paläolitischen Malerei Ostpaniens, in: Mora, P., Mora, L. and Philippot, P., Conservation of Wall Paintings, Quartier, 1, 111- 119.

Özgen, I. and Öztürk, J. (1996). The Lydian Treasure: Heritage Recovered, Republic of Turkey, Ministry of Culture, General Directorate of Monuments and Museums.

Perez-Rodriquez, J., Robador, M.D., Centeno, M.A., Siquenza, B., Duran, A. (2014). Wall Paintings Studied Using Raman Spectroscopy. Spectrochimica Acta. Volume 120. 602-609.

Peschlow-Bindokat A. (1998). The prehistoric rockpaintings of the Latmos Stonewatch Magazine 3, 27-29.

Pollard, A.M., Heron, C. (1996). Archaeological Chemistry, Royal Society of Chemistry, Cambridge, UK.

Rapp, G. (2002). Archaeomineralogy (Natural Science in Archaeology), Springer, Berlin Heidelberg New York.

RILEM, (1980). Research and Testing, Materials and Construction 13, Chapman and Hall, Paris.

Salmon, M.E. (1970). An X-Ray Fluorescence Method for Micro-Samples, IICAmericanGroup Technical Papers from 1968 through 1970; IIC-American Group: New York (1), 31-46.

Siddall, R. (1997). Lime, Cements, Mortars and Concretes; the Site of Ancient Corinth, Northern Peloponnese, Greece, 1. Preliminary Results from Morphologic

and Petrographic Analyses, Wiener Laboratory Internal Report, American School of Classical Studies, Athens.

Siddall, R. (2006). Pigments and Painting Techniques of Roman Artists, The Proceedings of the Royal Microscopical Society, Infocus Magazine, June 2, 18-31.

Siddall, R. and Çamurcuoğlu, D. (2016). Plastering Prehistory: Marl as a Unique Material to Cover, Maintain and Decorate the Neolithic Walls of Çatalhöyük, 4th Historic Mortars Conference, 482-489.

Siddall, R. (2018). Mineral Pigments in Archaeology: Their Analysis and the Range of Available Materials. *Minerals. 8,201.* 1-35.

Shackley, M.S, (2019). (Eds.), An Introduction to X-Ray Fluorescence (XRF) Analysis in Archaeology, X-Ray Fluorescence Spectrometry (XRF) in Geoarchaeology, Springer, New York.

Soykal-Alanyalı, F. (2016). Side Dionysos (?) Tapınağı Işığında Tiyatro ile Çevresinin Kentsel Değişimi ve Dönüşümü. *Olba (24),* 419-450.

Soykal-Alanyalı, F. (2016). Kaybolan Bir Kentin Yeniden Keşfinin Hikayesi, Mediterranean Journal of Humanities, VI/2 ,17-28.

Soykal-Alanyalı, F. S. (2017). Bir Kentin Kayboluşunun Hikayesi, Arkeoloji ve Sanat, 155: Mayıs-Ağustos, 187-196.

Şerifaki K. (2005). "Ayvalık Cunda Adası Taxiarhis Kilisesi Tarihi Duvar Resimlerinin Koruma Problemleri", Yüksek Lisans Tezi, İzmir Yüksek Teknoloji Enstitüsü, Mühendislik ve Fen Bilimleri Enstitüsü, İzmir.

Torraca, G. (1969). Deterioration Processes of Mural Paintings, Seminar on the Application of Science to the Conservation of Works of Art, Boston, 170-175.

Tunçoku, S.S. (2001). Characterization of Masonry Mortars Used in some Anatolian Seljuk Monuments in Konya, Beyşehir and Akşehir, Unpublished Ph.D. Thesis in Middle East Technical University, Ankara, Turkey, 10-15.

Vandenabeele, P., Bode, S., Alonso, A. Moens, L. (2005). Raman Spectroscopic Analysis of the Maya Wall Paintings in Ek'Balam, Mexico. *Spectrochimica Acta* Volume 61. Issue 10. 2349-2356.

Vitruvius, P.M. (1990). Mimarlık Üzerine On Kitap, The Ten Books On Architectura, (Çeviren: Suna Güven), Şevki Vanlı Mimarlık Vakfı Yayınları, Yapı Endüstri Merkezi, Ankara.

Wentwort, C.K., (1922). "A scale of Grade and Class Terms for Clastic Sediments", Journal of Geology Vol. 30, No. 5, pp. 377-392.

Wickens, D. (1984). Plaster, Render and Tiles, A.J. 4, 3-23.

Wooley, L. (1955). Alalakh, in: Mora, P., Mora, L. and Philippot, P., Conservation of Wall Paintings, Oxford, 228-231.

Yılmaz, F. (2008). Arkaik Dönem Batı Anadolu Resim Sanatı, Ege University, Social Sciences Institue, Unpublished PHD. Thesis.

Yıldırım, Ş. (2003). Side Antik Kentinin Dini Mimarisi, Unpublised PHD. Thesis in Anadolu University.

Young, C.A. and Miller, J.D. (2000). Effect of Temperature on Oleate Adsorption at a Calcite Surface: An FT-NIR/IRS Study and Review, International Journal of Miner Process, 331-350.

(https://www.ancient.eu/Altamira/

APPENDICES

A. Figures and Tables of the Thesis

SKT-S1

SKT-P1

SKT-S2

SKT-P2

SKT-S3

SKT-P3

SKT-S4

SKT-P4

SKT-S5

SKT-S6

SKT-P5

SKT-S7

SKT-P6

SKT-S8

SKT-P7

SKT-S9

SKT-P8

SKT-S10

SKT-P9

SKT-S11

SKT-P100

SKT-S12

SKT-P11

SKT-S13

SKT-P12

SKT-S14

SKT-P13

SKT-S15

SKT-P14

SKT-S16

SKT-P15

SKT-S17

SKT-P16

SKT-S19

SKT-P18

Figures A.1 Documentation of the Samples

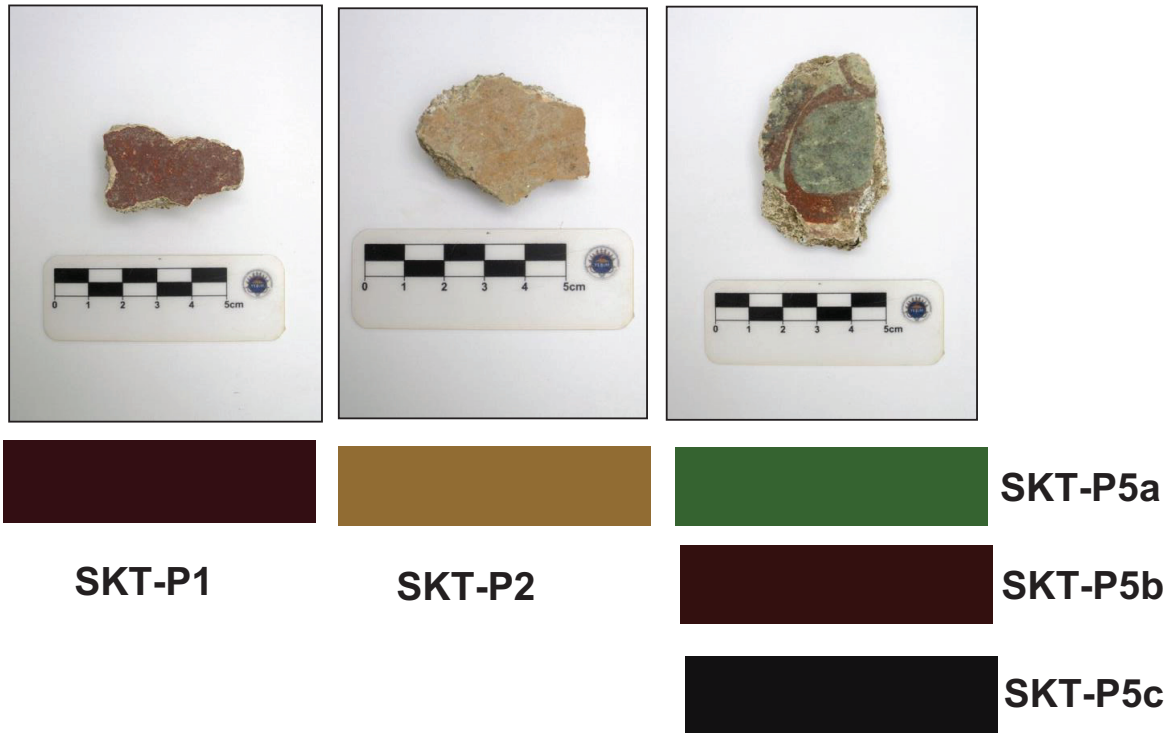

Figures A.2. Equivalent Colors of the Samples

Figures A.3. Sampling

Figures A.4. Thin Section Optical Microscopy Images

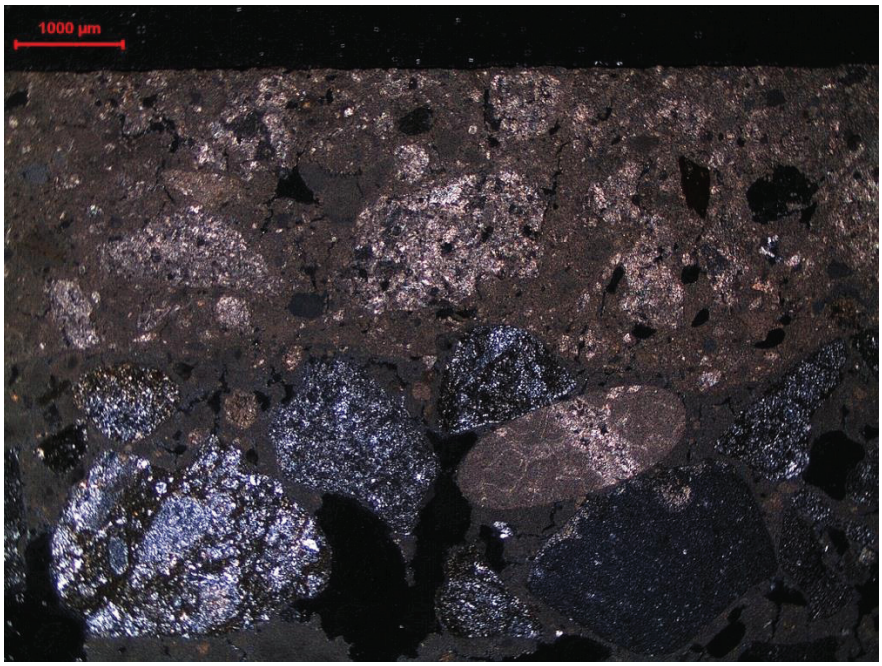

SKT-S1

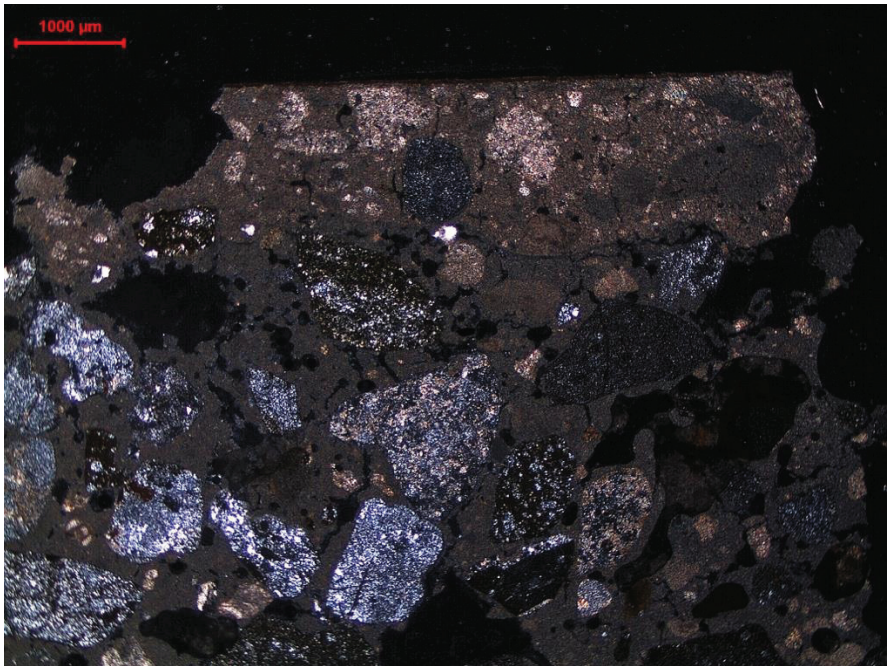

SKT-S2

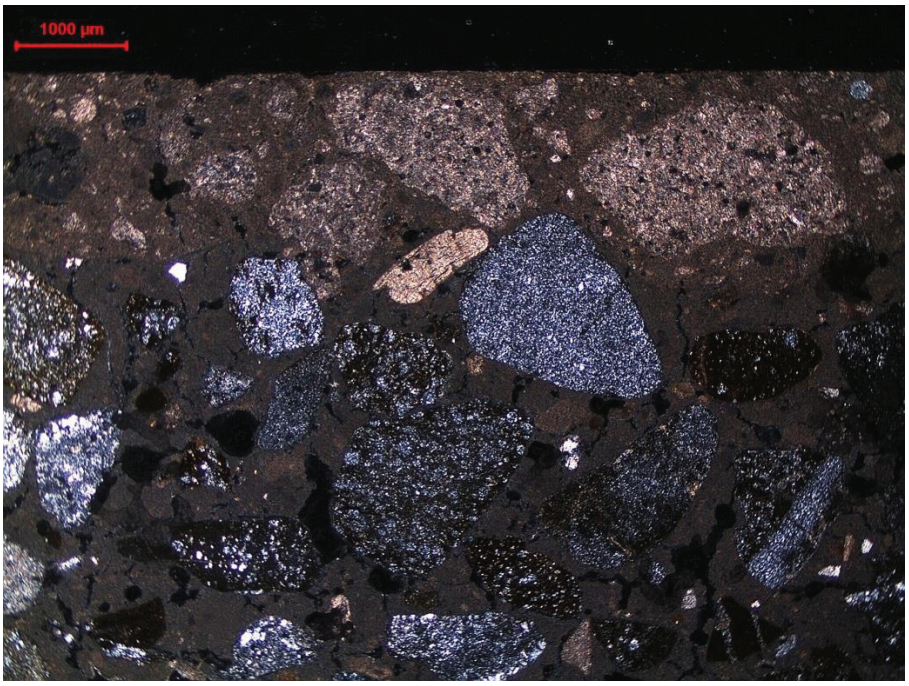

SKT-S3

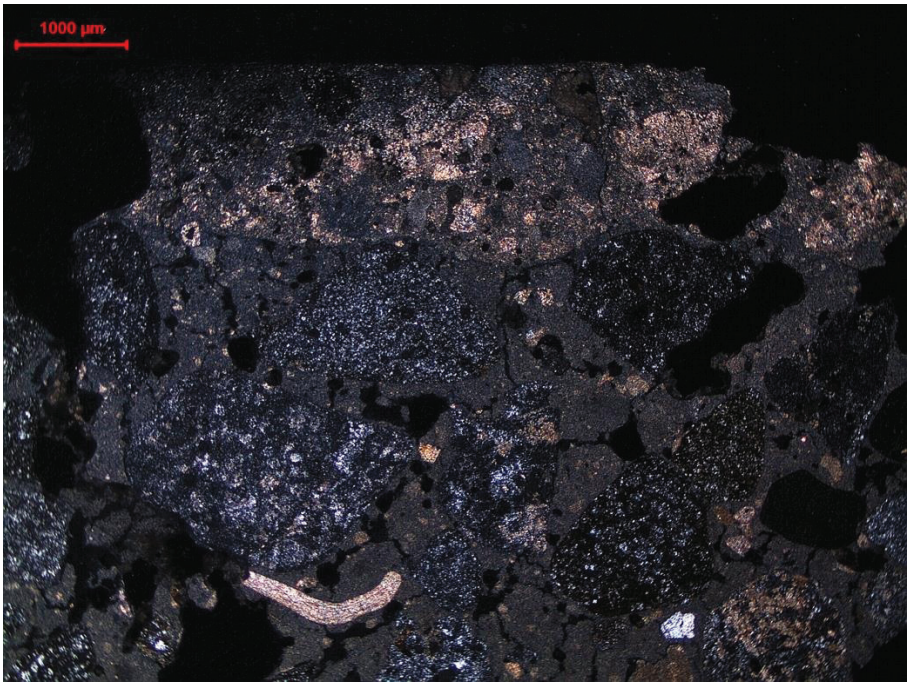

SKT-S4

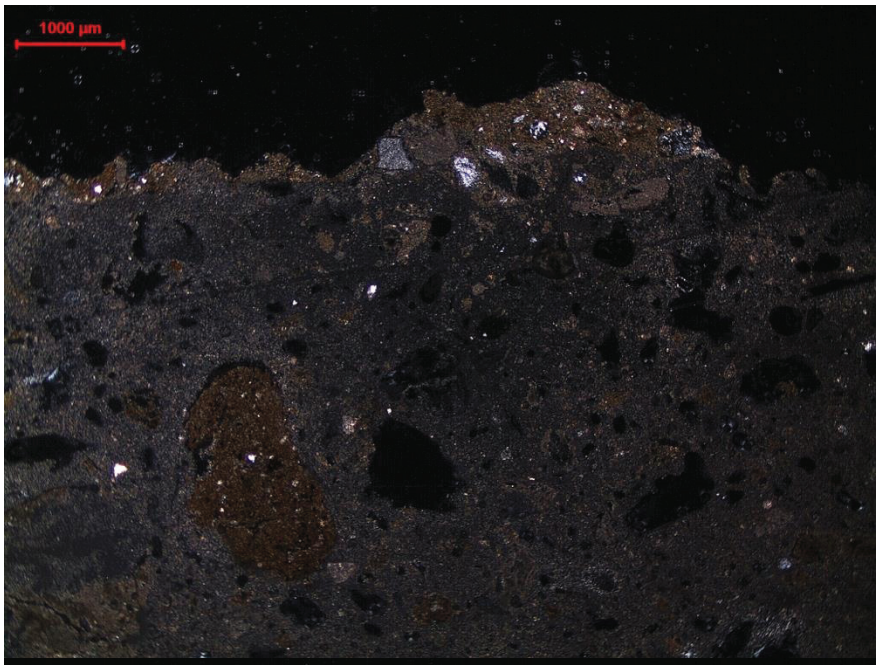

SKT-S5

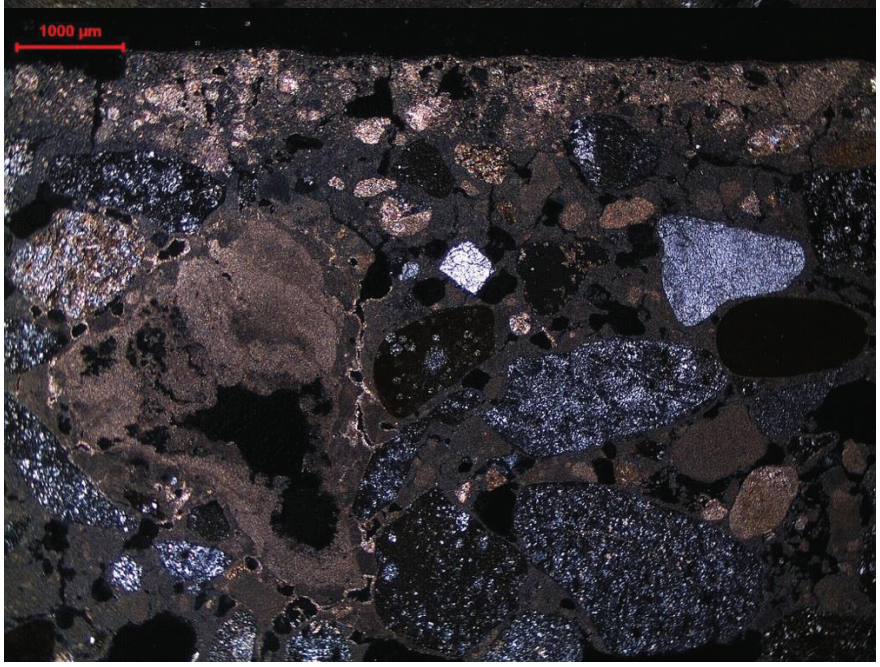

SKT-S6

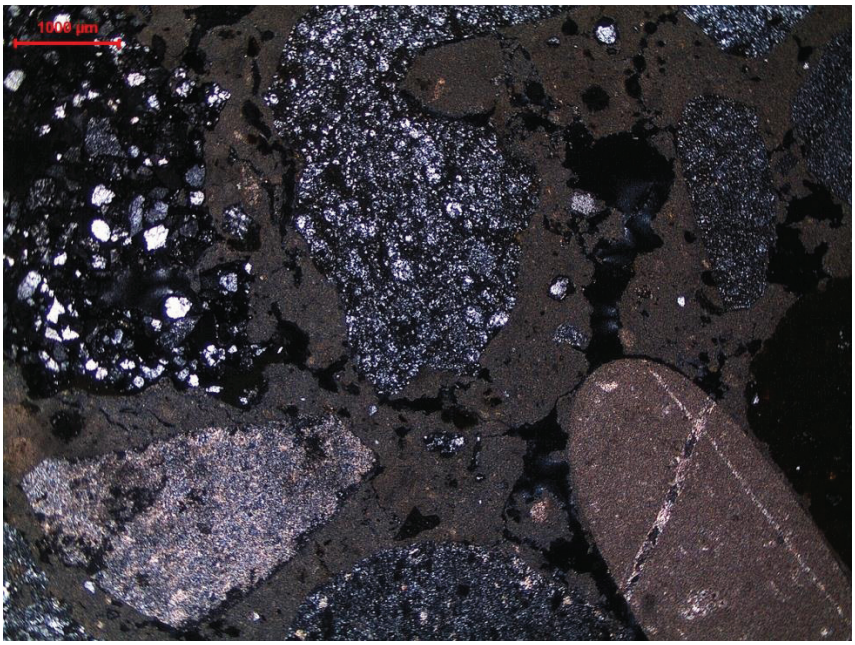

SKT-S7

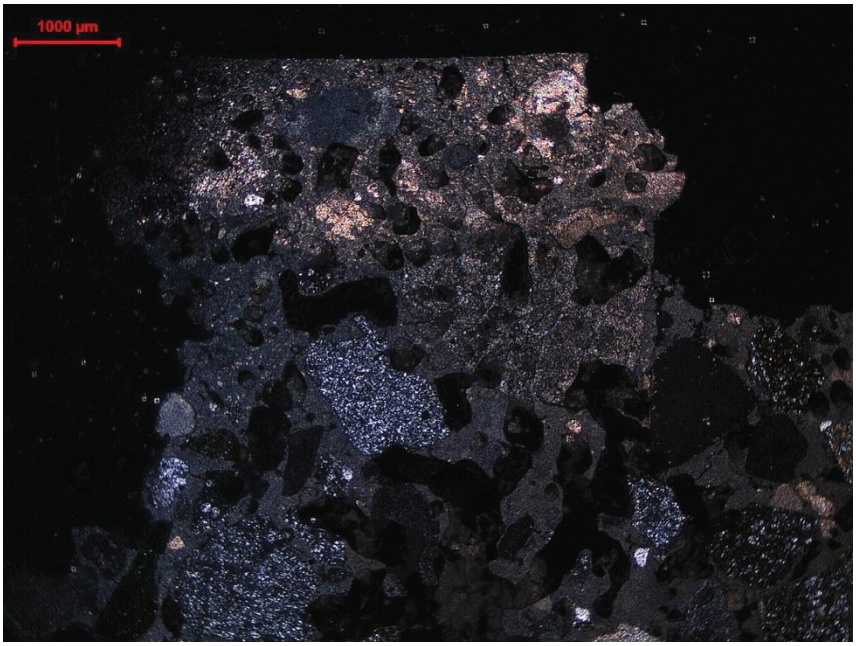

SKT-S8

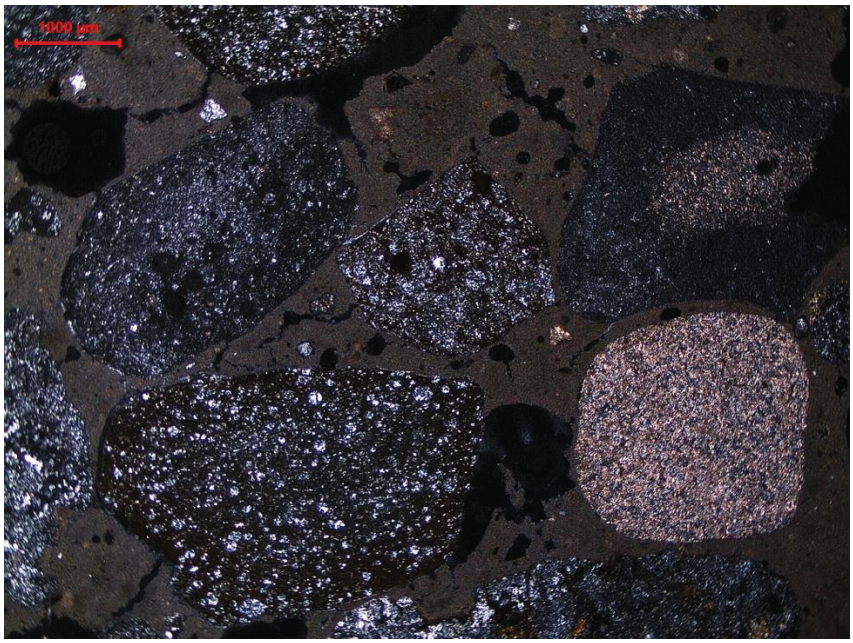

SKT-S9

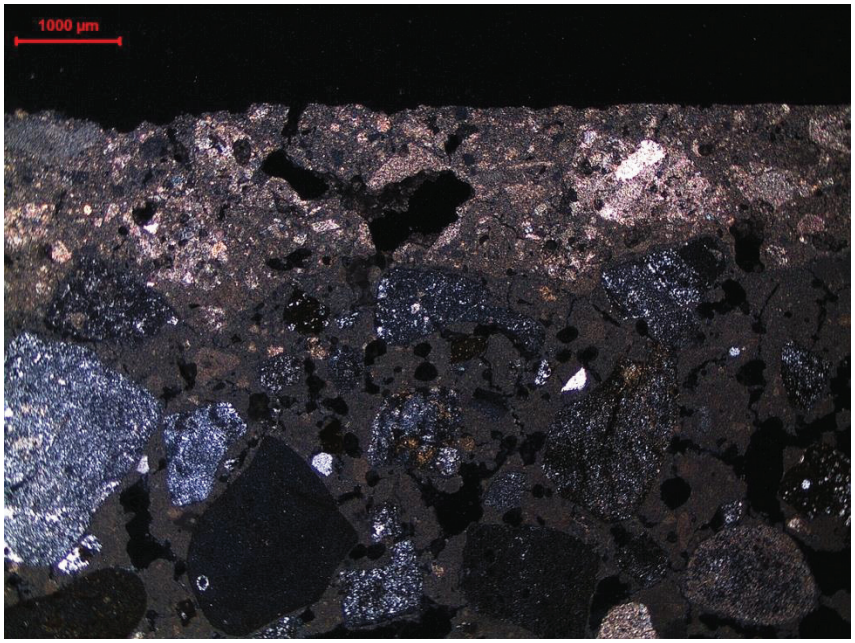

SKT-S10

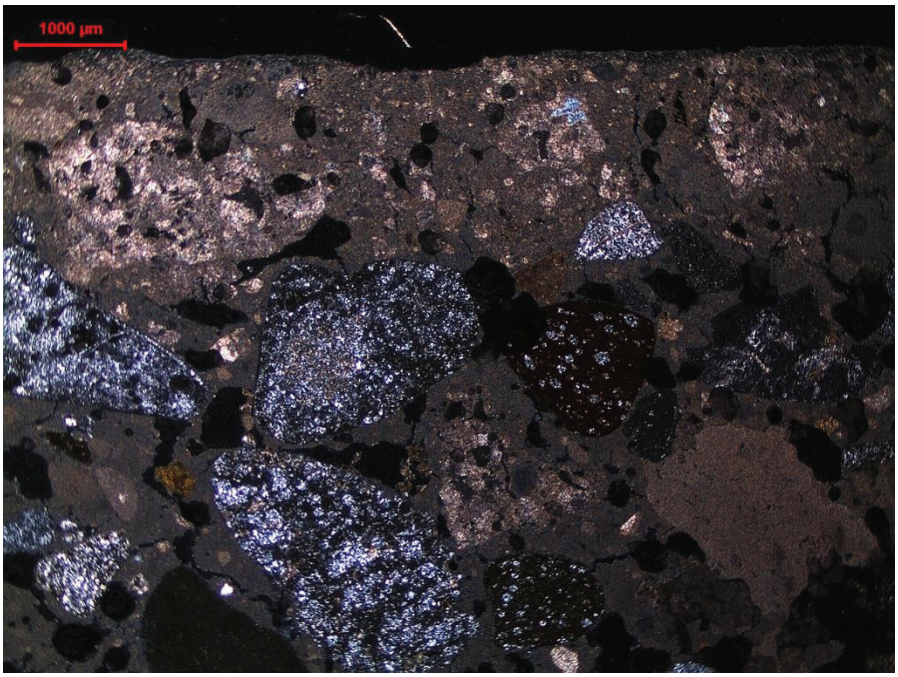

SKT-S11

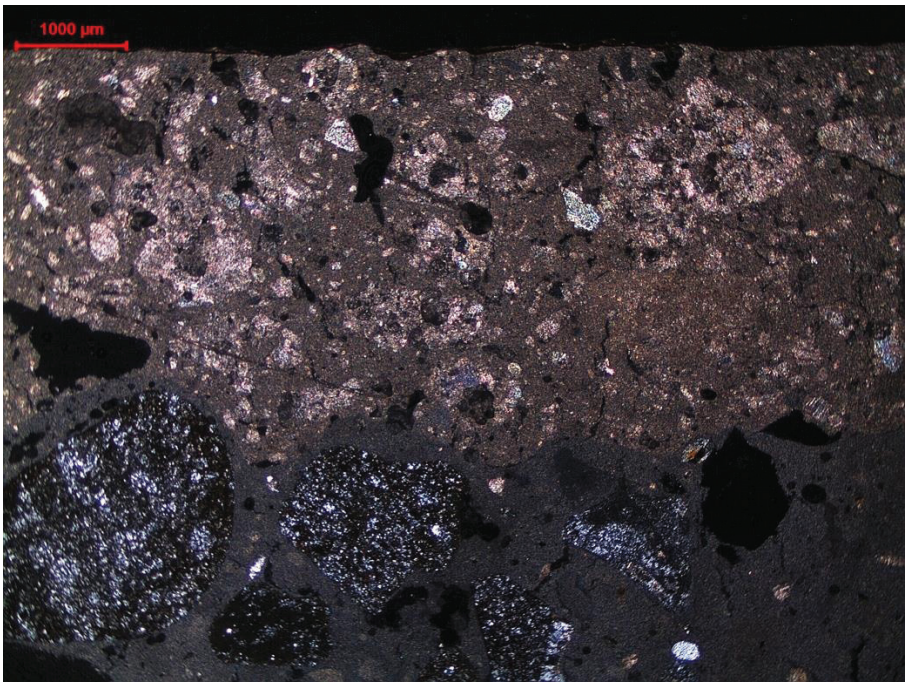

SKT-S12

Table A. 1 Gravimetric Analysis Results-Water Absorption Capacity

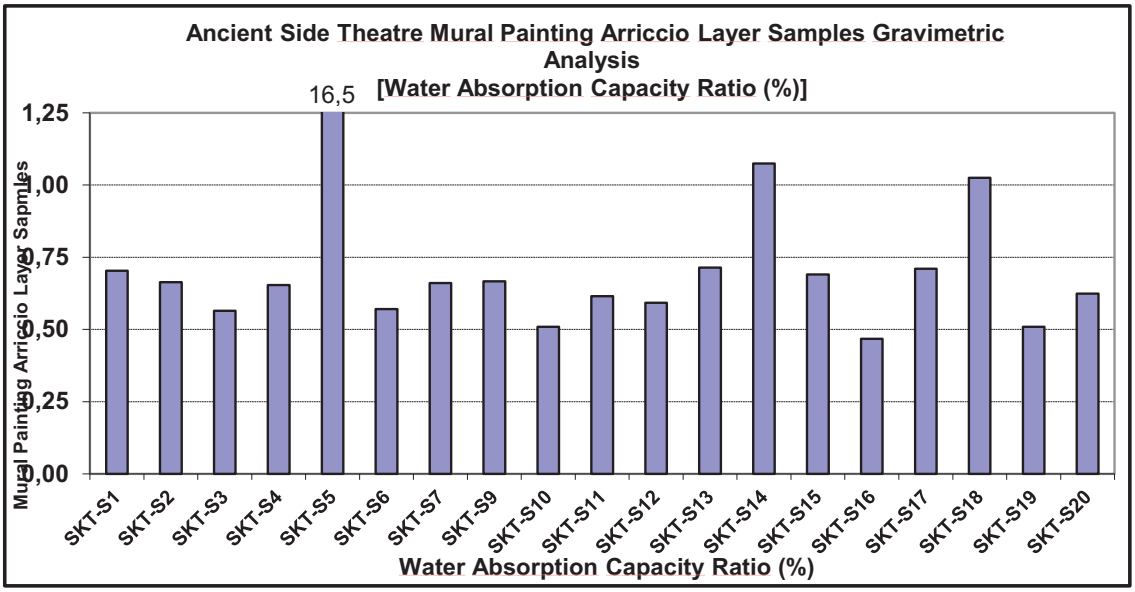

Table A.2. Gravimetric Analysis Results- Total Organic Carbon Ratio

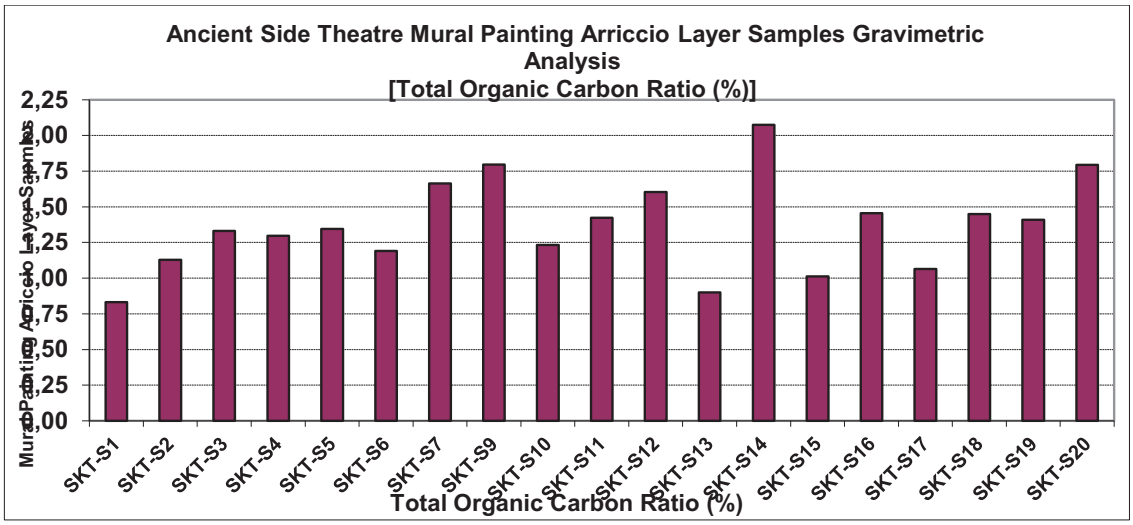

Table A.3.Gravimetric Analysis Results- Total Carbonate Ratio

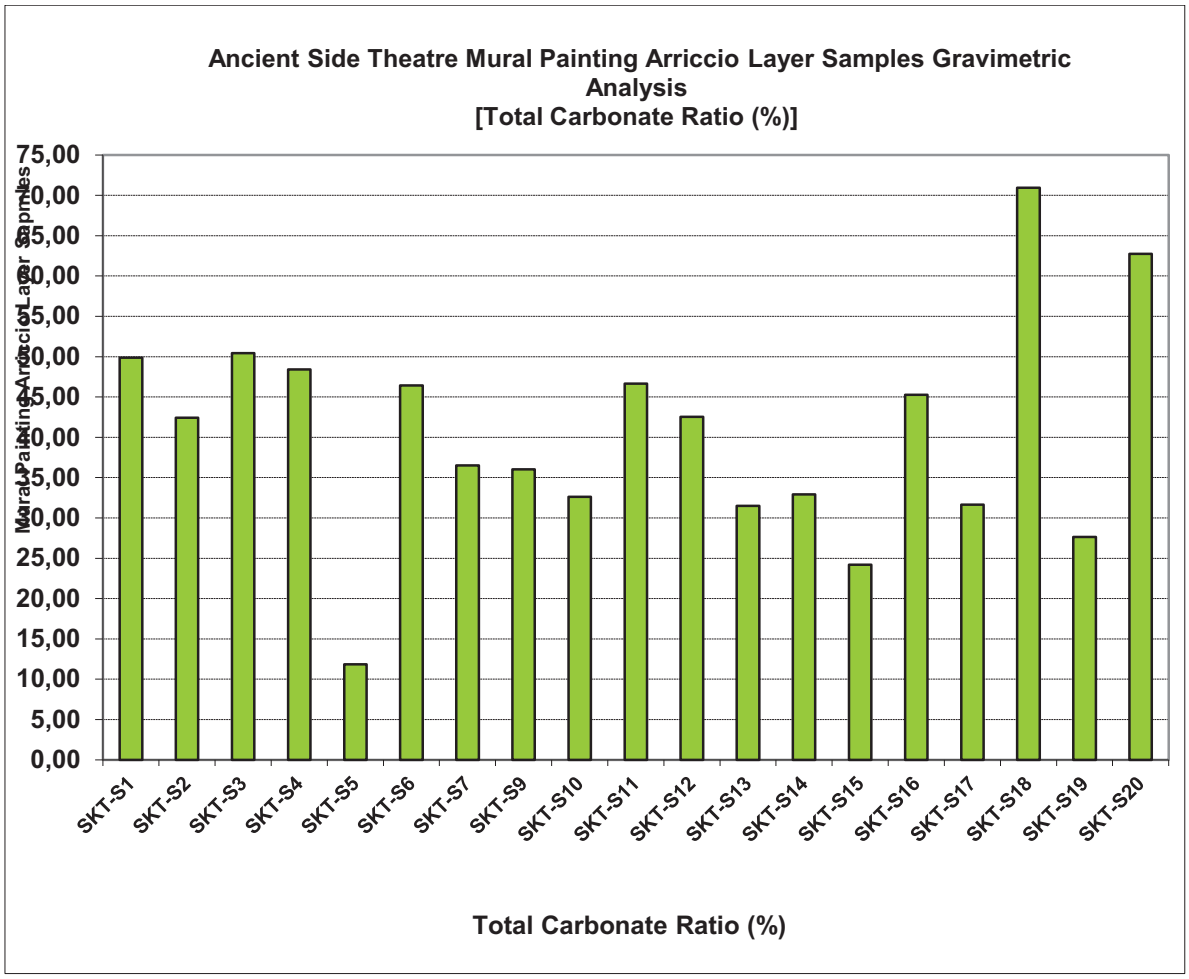

Table A.4.Acidic Aggregate & Binder Analysis

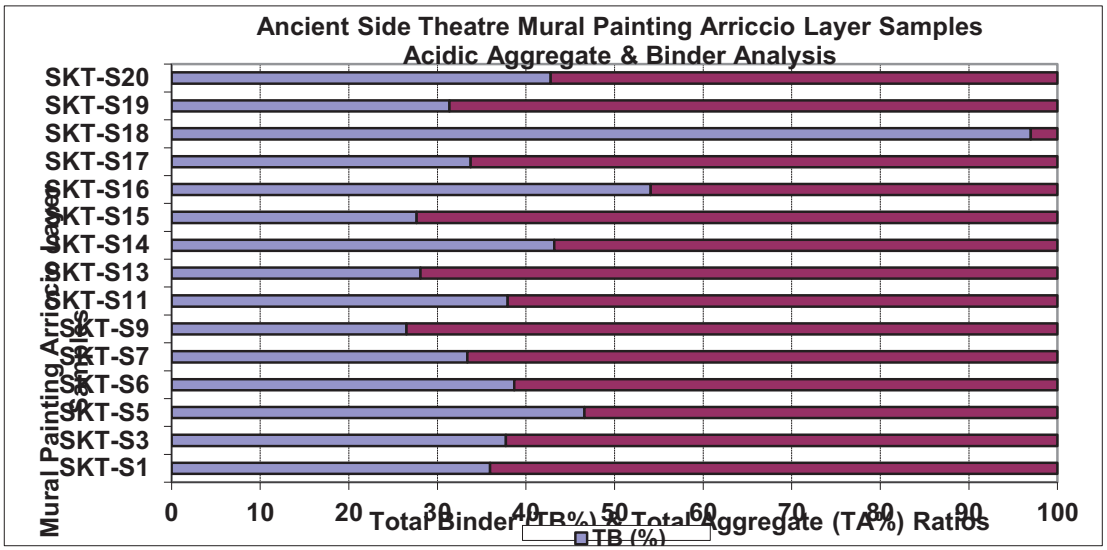

Table A.5.Aggregate Granulometry

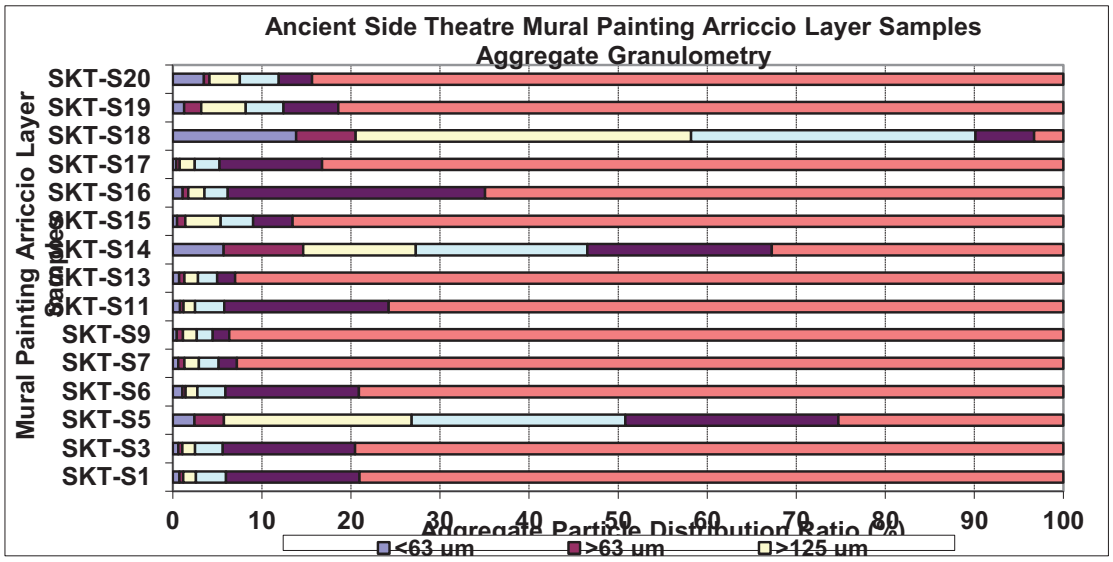

Table A.6 PED-XRF Results

Element	Conc.	SKT-S1	SKT-S2	SKT-S3	SKT-S4	SKT-S5	SKT-S6	SKT-S7	SKT-S9	SKT-S11	Average	SD
Na2O	%	0,041	0,056	0,050	0,050	0,120	0,049	0,049	0,047	0,046	0,049	0,02
MgO	%	0,438	0,088	0,178	0,125	0,271	0,075	0,102	0,154	0,231	0,185	0,12
Al2O3	%	1,567	0,598	0,763	0,706	0,954	0,843	1,129	1,449	0,371	0,931	0,39
SiO2	%	12,35	8,23	9,70	10,51	4,44	6,36	9,82	10,85	18,55	10,09	3,98
P2O5	%	0,134	0,103	0,115	0,096	0,148	0,123	0,132	0,118	0,099	0,118	0,02
SO3	%	0,108	0,124	0,133	0,269	34,97	0,202	0,239	0,161	0,136	0,171	11,60
Cl	%	0,066	0,080	0,072	0,073	0,001	0,069	0,097	0,043	0,065	0,063	0,03
K2O	%	0,492	0,310	0,300	0,300	0,341	0,303	0,361	0,425	0,256	0,343	0,07
CaO	%	34,15	42,59	46,60	42,95	32,27	51,07	45,18	47,83	41,51	42,68	6,14
TiO2	%	0,149	0,061	0,079	0,083	0,195	0,094	0,111	0,156	0,053	0,109	0,05
V2O5	%	0,006	0,005	0,005	0,005	0,002	0,007	0,004	0,003	0,001	0,004	0,00
Cr2O3	%	0,019	0,011	0,013	0,012	0,008	0,012	0,017	0,018	0,048	0,017	0,01
MnO	%	0,034	0,026	0,028	0,027	0,019	0,032	0,057	0,056	0,029	0,034	0,01
Fe2O3	%	1,242	0,703	0,722	0,776	0,696	0,765	1,187	1,457	0,797	0,927	0,29
LOI	%	49,20	47,01	41,24	44,02	25,57	40,00	41,52	37,23	37,81	40,40	6,83
Total	%	100,00	100,00	100,00	100,00	100,00	100,00	100,00	100,00	100,00	100,00	0,00
Co	µg/g	8,8	6,5	6,5	8,5	20	16	30,5	11	14	13,5	7,82
Ni	µg/g	37,1	20,5	21	19,6	18,9	21,1	28,1	35,9	16,9	24,3	7,54
Cu	µg/g	60,5	23,1	14,3	11,7	5,5	11,7	29,8	12,7	48,3	24,2	18,79
Zn	µg/g	17,8	14,8	11,2	13,8	6	12,5	15,9	19,6	30,4	15,8	6,75
Ga	µg/g	3,2	2,9	3	1,8	4,3	3,7	2,5	3,6	0,7	2,9	1,08
Ge	µg/g	0,4	0,4	0,4	0,5	0,4	0,4	0,4	0,4	0,4	0,4	0,03
As	µg/g	6,8	4	5,6	4,6	1,1	2,6	14,6	19,7	6,7	7,3	6,01
Se	µg/g	0,3	0,3	0,3	0,5	0,3	0,3	0,3	0,3	0,3	0,3	0,07
Br	µg/g	5	4,7	5,4	4,4	1	3,4	5,3	4,5	2,9	4,1	1,42
Rb	µg/g	17,9	7,6	8,6	10,1	10,8	9,1	9,7	13,6	7,5	10,5	3,32
Sr	µg/g	205	222,1	215,2	199,7	289,1	227,1	267,4	266,6	185	230,8	35,50
Y	µg/g	5,2	2,9	4	1,7	1,5	4,2	7,1	8,9	3,3	4,3	2,44
Zr	µg/g	54,7	16	24,4	15,3	19,1	37,3	35,4	49,4	16,8	29,8	15,02
Nb	µg/g	4	3,7	3,1	2,9	2,9	6,1	3,1	5,7	3	3,8	1,23
Mo	µg/g	2,5	3,6	2,9	3,1	2,9	3,1	3,8	3	2,9	3,1	0,39
Cd	µg/g	0,7	1,3	0,9	1,1	0,9	1,1	1	1	0,9	1,0	0,17
In	µg/g	0,7	1,2	0,9	1	0,9	0,9	0,9	0,9	0,8	0,9	0,14
Sn	µg/g	0,9	1,6	1,1	1,2	1	1	1	1,1	1	1,1	0,21
Sb	µg/g	0,8	1,5	1	1,2	1,1	1	0,9	1,9	1	1,2	0,34
Te	µg/g	1	2	1,4	1,6	2,7	1,3	1,4	1,2	1,3	1,5	0,52
I	µg/g	4,2	3,1	2,5	2,8	2,4	2,2	2,5	3,2	2,4	2,8	0,62
Cs	µg/g	3,3	6,7	4,4	5,2	4,3	4	4,4	4,1	7,7	4,9	1,42
Ba	µg/g	62,5	123,3	75,1	65,2	57,3	51,3	125,3	115,1	58,1	81,5	30,63
La	µg/g	6,3	33,3	9,6	26,7	16,4	8,8	14,3	8,7	25,7	16,6	9,67
Ce	µg/g	18,8	21	13	16	30,4	13,2	13	12	16,5	17,1	5,82
Hf	µg/g	3,7	3,7	3,4	7,3	2,5	2,2	3,5	3,1	4,5	3,8	1,49
Ta	µg/g	4,4	3,6	3,1	3,1	2,4	3,2	3,8	3,3	4,4	3,5	0,65
W	µg/g	2,4	2,5	2,3	2,4	2	2,3	2,5	2,8	2,4	2,4	0,21
Hg	µg/g	0,7	0,8	0,7	1	0,7	0,8	0,8	0,8	0,8	0,8	0,09
Tl	µg/g	0,7	0,7	0,9	2,1	0,7	0,8	0,9	0,9	0,9	1,0	0,44
Pb	µg/g	40,6	26,4	34,6	1184	10,3	65	36,8	15,2	121,7	170,5	381,52
Bi	µg/g	0,4	0,7	0,7	1,9	0,6	0,8	0,7	0,7	0,8	0,8	0,43
Th	µg/g	2,4	0,9	2,2	6,1	2,1	1,5	2	2,6	1,4	2,4	1,50
U	µg/g	7,2	7,9	8,4	7,6	8,3	8,6	8,7	9,5	8,4	8,3	0,67

Table A.7. PED-XRF Plot

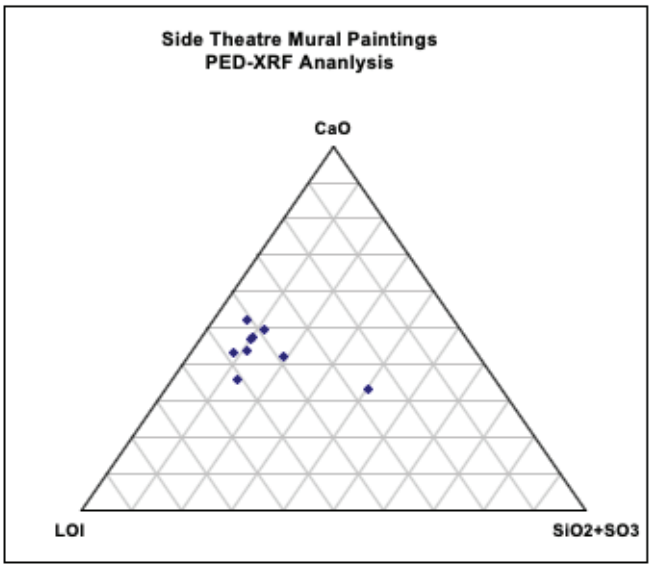

Element	SKT-S1	SKT-S2	SKT-S3	SKT-S4	SKT-S5	SKT-S6	SKT-S7	SKT-S9	SKT-S11
SiO2	12,35	8,23	9,70	10,51	4,44	6,36	9,82	10,85	18,55
SO3	0,108	0,124	0,133	0,269	34,97	0,202	0,239	0,161	0,136
CaO	34,15	42,59	46,60	42,95	32,27	51,07	45,18	47,83	41,51
LOI	49,20	47,01	41,24	44,02	25,57	40,00	41,52	37,23	37,81

Table A.8. SEM-EDX SKT-P4

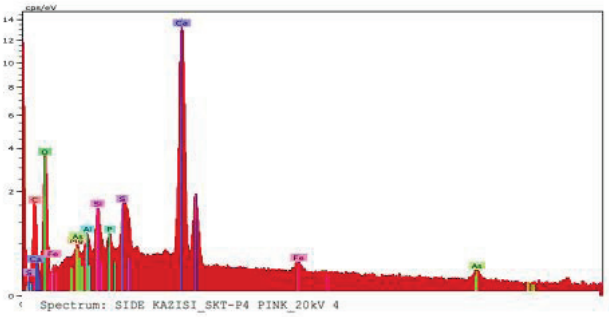

Spectrum: SIDE KAZISI_SKT-P4 PINK_20kV 4

Element	unn. C [wt.%]	norm. C [wt.%]	Atom. C [at.%]	Compound	norm. Comp. C [wt.%]	Error (3 Sigma) [wt.%]
Carbon	0.00	0.00	0.00		0.00	0.00
Oxygen	18.98	31.02	53.12		0.00	7.56
Calcium	34.33	56.11	38.36	CaO	78.51	3.10
Aluminium	0.49	0.81	0.82	Al2O3	1.52	0.16
Silicon	1.28	2.09	2.04	SiO2	4.48	0.25
Magnesium	0.14	0.23	0.26	MgO	0.39	0.11
Phosphorus	0.34	0.55	0.49	P2O5	1.26	0.13
Sulfur	1.79	2.92	2.50	SO3	7.30	0.28
Iron	0.61	0.99	0.49	FeO	1.28	0.16
Arsenic	3.23	5.27	1.93		5.27	0.53
Total:	61.18	100.00	100.00			

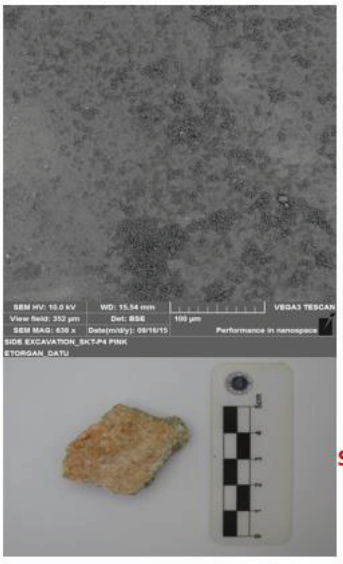

Table A.9. SEM-EDX SKT-P6

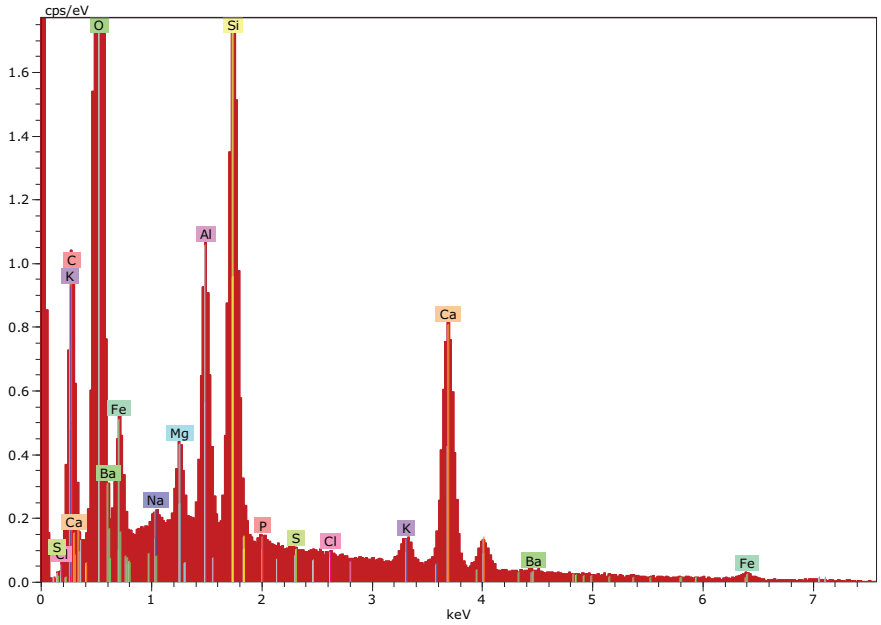

Spectrum: SIDE EXCAVATION_SKT-P6 RED 5

Element	Series	unn. C [wt.%]	norm. C [wt.%]	Atom. C [at.%]	Error (1 Sigma) [wt.%]
Carbon	K-series	10.49	9.44	14.97	1.53
Oxygen	K-series	60.58	54.47	64.88	6.94
Sodium	K-series	0.68	0.61	0.51	0.07
Magnesium	K-series	1.50	1.35	1.06	0.11
Aluminium	K-series	4.35	3.91	2.76	0.23
Silicon	K-series	11.64	10.47	7.10	0.51
Calcium	K-series	15.32	13.77	6.55	0.55
Iron	K-series	3.18	2.86	0.97	0.26
Potassium	K-series	1.39	1.25	0.61	0.08
Chlorine	K-series	0.24	0.21	0.12	0.04
Sulfur	K-series	0.22	0.19	0.12	0.04
Phosphorus	K-series	0.36	0.32	0.20	0.04
Barium	L-series	1.29	1.16	0.16	0.10
	Total:	111.23	100.00	100.00	

Table A.10. Mikro-XRF Results

Element	Dimension	SKT-P1	SKT-P2	SKT-P3a	SKT-P3b	SKT-P3c	SKT-P3d	SKT-P4	SKT-P5a	SKT-P5b	SKT-P5c	SKT-P5d	SKT-P6	SKT-P7a	SKT-P7b	SKT-P8	SKT-P9a	SKT-P9b
Al	%	5,56	5,97	4,90	4,50	0,72	4,69	0,740	5,26	5,19	4,51	5,47	5,14	5,61	5,97	5,23	5,52	5,45
Ti	%	0,815	0,036	0,015	0,012	0,010	0,013	0,008	0,026	0,014	0,006	0,020	0,032	0,011	0,020	0,047	0,044	0,600
V	%	0,360	0,005	0,004	0,004	0,006	0,004	0,006	0,005	0,004	0,004	0,004	0,006	0,004	0,004	0,006	0,007	0,248
Cr	%	0,009	0,003	0,030	0,030	0,004	0,030	0,004	0,003	0,030	0,030	0,030	0,005	0,030	0,030	0,010	0,003	0,007
Mn	%	0,033	0,025	0,025	0,025	0,005	0,025	0,006	0,025	0,025	0,025	0,025	0,023	0,025	0,025	0,011	0,025	0,023
Fe	%	0,837	0,594	0,077	0,125	0,067	0,073	0,046	0,517	0,084	0,032	0,112	1,85	0,052	0,114	1,67	0,369	0,638
Co	%	0,004	0,004	0,020	0,020	0,002	0,020	0,002	0,003	0,020	0,020	0,020	0,006	0,020	0,020	0,005	0,003	0,004
Ni	%	0,015	0,015	0,015	0,015	0,002	0,015	0,002	0,015	0,015	0,015	0,015	0,015	0,015	0,015	0,015	0,015	0,015
Cu	%	0,010	0,022	0,010	0,010	0,008	0,010	0,008	0,010	0,010	0,010	0,010	0,004	0,010	0,010	0,010	0,010	0,010
Zn	%	0,001	0,010	0,010	0,010	0,001	0,010	0,001	0,010	0,010	0,010	0,010	0,010	0,010	0,010	0,001	0,010	0,010
Ga	%	0,010	0,010	0,001	0,001	0,003	0,001	0,009	0,001	0,010	0,010	0,010	0,010	0,010	0,010	0,010	0,001	0,010
Zr	%	0,050	0,050	0,050	0,050	0,050	0,050	0,050	0,050	0,050	0,050	0,050	0,050	0,050	0,050	0,050	0,050	0,050
Nb	%	0,059	0,062	0,059	0,056	0,064	0,059	0,059	0,060	0,054	0,051	0,056	0,081	0,054	0,059	0,071	0,061	0,059
Mo	%	0,050	0,070	0,066	0,062	0,114	0,068	0,120	0,070	0,059	0,057	0,063	0,075	0,059	0,067	0,065	0,066	0,050
Rh	%	0,002	0,002	0,002	0,002	0,002	0,002	0,002	0,002	0,002	0,002	0,002	0,002	0,002	0,002	0,002	0,002	0,002
Pd	%	0,003	0,003	0,003	0,003	0,006	0,003	0,006	0,003	0,003	0,003	0,003	0,004	0,003	0,003	0,004	0,003	0,003
Ag	%	0,004	0,004	0,004	0,004	0,007	0,004	0,007	0,004	0,003	0,003	0,004	0,005	0,003	0,004	0,004	0,004	0,004
Cd	%	0,050	0,050	0,050	0,050	0,009	0,050	0,009	0,050	0,050	0,050	0,050	0,005	0,050	0,050	0,050	0,050	0,050
In	%	0,005	0,005	0,005	0,005	0,010	0,005	0,010	0,005	0,005	0,004	0,005	0,007	0,005	0,006	0,006	0,006	0,006
Sn	%	0,007	0,007	0,007	0,006	0,013	0,007	0,014	0,006	0,006	0,006	0,006	0,008	0,006	0,007	0,008	0,007	0,007
Sb	%	0,010	0,010	0,010	0,009	0,018	0,010	0,018	0,010	0,009	0,009	0,009	0,012	0,009	0,011	0,011	0,010	0,010
W	%	0,025	0,003	0,003	0,003	0,025	0,003	0,025	0,003	0,025	0,025	0,025	0,003	0,025	0,025	0,003	0,003	0,025
Ir	%	0,001	0,001	0,001	0,001	0,001	0,001	0,001	0,001	0,001	0,001	0,001	0,001	0,001	0,001	0,001	0,001	0,001
Pt	%	0,020	0,020	0,020	0,020	0,020	0,020	0,020	0,020	0,020	0,020	0,020	0,020	0,020	0,020	0,020	0,020	0,020
Au	%	0,020	0,020	0,020	0,020	0,020	0,020	0,020	0,020	0,020	0,020	0,020	0,020	0,020	0,020	0,020	0,020	0,020
Pb	%	0,047	0,043	0,341	0,296	2,84	0,265	2,72	0,160	0,165	0,214	0,133	0,039	0,020	0,005	0,028	0,226	0,089
Toplam	%	8,01	7,04	5,75	5,34	4,03	5,46	3,91	6,34	5,88	5,19	6,17	7,43	6,12	6,56	7,36	6,53	7,41

Element	Dimension	SKT-P10	SKT-P11a	SKT-P11b	SKT-P12	SKT-P13	SKT-P14	SKT-P15a	SKT-P15b	SKT-P15c	SKT-P15d	SKT-P15e	SKT-P16a	SKT-P16b	SKT-P17a	SKT-P17b	SKT-P17c	SKT-P17d	SKT-P18	SKT-P19a	SKT-P19b	SKT-P19c
Al	%	5,17	5,82	5,71	5,13	5,15	5,24	5,49	5,39	5,42	5,65	4,26	5,14	4,99	3,91	4,28	4,63	4,67	4,72	5,49	4,41	4,03
Ti	%	0,038	0,060	0,063	0,031	0,040	0,064	0,014	0,009	0,015	0,009	0,021	0,008	0,021	0,013	0,015	0,016	0,042	0,043	0,013	0,011	0,005
V	%	0,005	0,006	0,006	0,005	0,004	0,005	0,006	0,004	0,004	0,004	0,005	0,004	0,004	0,007	0,007	0,005	0,007	0,005	0,005	0,004	0,035
Cr	%	0,003	0,004	0,005	0,004	0,030	0,003	0,004	0,030	0,030	0,030	0,004	0,030	0,030	0,005	0,005	0,024	0,050	0,003	0,004	0,003	0,030
Mn	%	0,012	0,014	0,012	0,010	0,025	0,025	0,007	0,025	0,025	0,025	0,007	0,025	0,025	0,006	0,005	0,004	0,012	0,030	0,011	0,025	0,025
Fe	%	0,673	1,32	2,17	1,26	0,210	0,433	1,55	0,146	0,260	0,071	1,14	0,135	0,309	4,64	3,30	0,273	0,719	0,583	0,811	0,134	0,086
Co	%	0,004	0,005	0,006	0,005	0,002	0,003	0,005	0,020	0,002	0,020	0,005	0,020	0,003	0,008	0,007	0,003	0,004	0,003	0,004	0,002	0,020
Ni	%	0,015	0,015	0,015	0,015	0,015	0,015	0,015	0,015	0,015	0,015	0,015	0,015	0,015	0,002	0,002	0,002	0,015	0,015	0,015	0,015	0,015
Cu	%	0,010	0,010	0,010	0,010	0,010	0,010	0,010	0,010	0,010	0,010	0,010	0,010	0,010	0,004	0,012	0,235	0,012	0,010	0,010	0,004	0,010
Zn	%	0,010	0,010	0,002	0,010	0,010	0,010	0,001	0,010	0,010	0,010	0,010	0,010	0,010	0,001	0,001	0,008	0,010	0,010	0,010	0,273	0,077
Ga	%	0,010	0,010	0,010	0,010	0,010	0,010	0,010	0,010	0,010	0,010	0,010	0,010	0,010	0,001	0,001	0,001	0,001	0,010	0,010	0,010	0,010
Zr	%	0,050	0,050	0,050	0,050	0,050	0,050	0,050	0,050	0,050	0,050	0,050	0,050	0,050	0,050	0,050	0,050	0,050	0,050	0,050	0,050	0,050
Nb	%	0,059	0,065	0,067	0,065	0,060	0,076	0,069	0,061	0,053	0,056	0,061	0,063	0,062	0,071	0,087	0,089	0,068	0,080	0,065	0,076	0,070
Mo	%	0,064	0,070	0,068	0,064	0,058	0,065	0,076	0,060	0,058	0,058	0,068	0,060	0,060	0,066	0,090	0,098	0,068	0,065	0,066	0,061	0,067
Rh	%	0,002	0,002	0,002	0,002	0,002	0,002	0,002	0,002	0,002	0,002	0,002	0,002	0,002	0,002	0,002	0,002	0,002	0,002	0,002	0,002	0,002
Pd	%	0,003	0,003	0,004	0,004	0,003	0,003	0,004	0,003	0,003	0,003	0,003	0,003	0,003	0,005	0,007	0,004	0,003	0,004	0,003	0,003	0,003
Ag	%	0,004	0,004	0,004	0,004	0,003	0,004	0,004	0,004	0,003	0,003	0,004	0,004	0,004	0,005	0,005	0,005	0,004	0,004	0,004	0,004	0,004
Cd	%	0,050	0,050	0,050	0,050	0,050	0,050	0,050	0,050	0,050	0,050	0,050	0,050	0,050	0,006	0,006	0,006	0,050	0,050	0,050	0,050	0,050
In	%	0,005	0,005	0,006	0,006	0,005	0,005	0,006	0,005	0,005	0,005	0,005	0,005	0,005	0,007	0,008	0,007	0,006	0,006	0,006	0,005	0,005
Sn	%	0,006	0,007	0,008	0,007	0,006	0,007	0,008	0,006	0,006	0,006	0,006	0,007	0,006	0,008	0,009	0,008	0,007	0,008	0,007	0,006	0,006
Sb	%	0,010	0,010	0,011	0,011	0,009	0,010	0,011	0,009	0,009	0,009	0,010	0,009	0,010	0,012	0,013	0,012	0,010	0,011	0,011	0,009	0,009
W	%	0,025	0,003	0,003	0,003	0,025	0,003	0,003	0,025	0,025	0,025	0,003	0,025	0,003	0,003	0,004	0,025	0,003	0,003	0,003	0,025	0,025
Ir	%	0,001	0,001	0,001	0,001	0,001	0,001	0,001	0,001	0,001	0,001	0,001	0,001	0,001	0,001	0,001	0,001	0,001	0,001	0,001	0,001	0,001
Pt	%	0,020	0,020	0,020	0,020	0,020	0,020	0,020	0,020	0,020	0,020	0,020	0,020	0,020	0,020	0,020	0,020	0,020	0,020	0,020	0,020	0,020
Au	%	0,020	0,020	0,020	0,020	0,020	0,020	0,020	0,020	0,020	0,020	0,020	0,020	0,020	0,020	0,020	0,020	0,020	0,020	0,020	0,020	0,020
Pb	%	0,002	0,003	0,037	0,023	0,002	0,002	0,036	0,002	0,002	0,002	0,013	0,002	0,002	0,388	0,184	0,190	0,255	0,003	0,079	0,014	0,005
Toplam	%	6,27	7,58	8,36	6,82	5,82	6,14	7,47	5,99	6,11	6,16	5,80	5,73	5,73	9,26	8,14	5,74	6,11	5,76	6,77	5,24	4,68

Table A.11. Raman Spectroscopy SKT-P12